
Università degli Studi di Padova

Dipartimento di Ingegneria dell'Informazione


Master Thesis in ICT For Internet and Multimedia

# An ns-3 Module for Non-Terrestrial Network (NTN) Simulation: Implementation, Design and Performance Evaluation


Master Candidate

**Mattia Sandri**

**Student ID 2021425**

Supervisor

**Marco Giordani**

**University of Padova**

Co-supervisor

**Matteo Pagin**

**University of Padova**



Academic Year 2022/2023

# Abstract

While the 5th generation (5G) of mobile networks has landed in the commercial area, with features such as millimeter waves already being deployed, there still are other functionalities to be investigated, for example non-terrestrial networks (NTN). In this context, satellite-based communications offer new opportunities for future research and applications, such as providing connectivity to remote or otherwise unconnected areas, complementing terrestrial networks to reduce connection downtime, as well as increasing traffic efficiency in hot spot areas. This thesis implements the 3rd generation partnership project (3GPP) channel model for NTNs, which introduces an ad-hoc characterization of the attenuation of the signal in the space scenario, as well as new challenges for the whole protocol stack, including those associated with latency and coverage constraints, compared to terrestrial network. In such regard, we extend the ns-3 simulator with new modules to implement the attenuation of the signal due to atmospheric gases and scintillation and a new mobility model to account for the Geocentric Cartesian coordinate system of spaceborne vehicles. We evaluate the performance of the system based on full-stack end-to-end simulations, and provide guidelines on possible future developments.

# Contents

# Chapter 1

# Introduction

Since the wide adoption of cellular networks started at the end of the last century, the number of connected users has steadily grown, together with the capabilities provided by wireless networks. Mobile data traffic has reached 100EB/month in 2022, showing an increase of 40% between the Q2 of 2021 and the Q2 of 2022, according to the latest Ericsson Mobilty Report [1]. This trend is driven by the increase in mobile users subscriptions simultaneously with the increased per-user traffic, and is not expected to change in the near future, as reported in [2] and shown in figure 1.1.

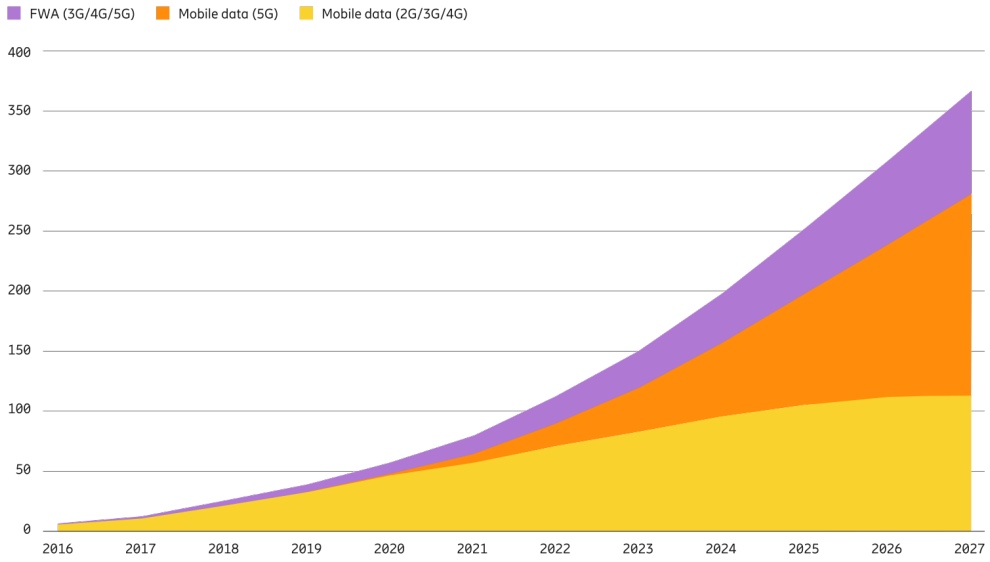


Figure 1.1: Global mobile traffic in EB per month. Figure from [1]

This, together with the rise of new use case scenarios in which the adoption of wireless communication systems are needed, such as machine to machine (M2M) and vehicle to everything (V2X) applications, poses new challenges in terms of system capacity as well as network coverage and service reliability. In this context, the research is investigating the

adoption of non-terrestrial networks (NTN), and the Third Generation Partnership Program (3GPP) has consolidated the possible use of NTN into the new radio (NR) standard in their latest Technical Release 17 [3].

NTN can offer new opportunities in terms of expanding already existing ground-based cellular systems, providing broadband coverage to rural regions where it would be otherwise not feasible to install cellular towers, enabling cost-effective connections in remote areas of the world. Moreover, the introduction of spaceborne/aerial vehicle, can complement ground infrastructures increasing service continuity and reliability of existing networks [4].

However, transmission using spaceborne/aerial vehicles introduces new challenges with respect to a terrestrial base station, namely:

- Increased path loss (PL) due to longer propagation distances
- Additional attenuation factors from the atmosphere, such as scintillation, rain and clouds
- Doppler shift, caused by the orbital velocity of the satellite
- Additional time delay, mainly for propagation

While satellite constellations have been used to provide phone service and internet access throughout the 1990s [5], their use was extremely limited due to high latency times and low bandwidth capabilities. Moreover, satellite communication was mainly provided by geostationary equatorial orbit (GEO) satellites, orbiting at 35'786 km and leading to huge delays. GEO orbits where chosen because of the wider coverage area offered, requiring less satellite launches and allowing for commercially feasible costs.

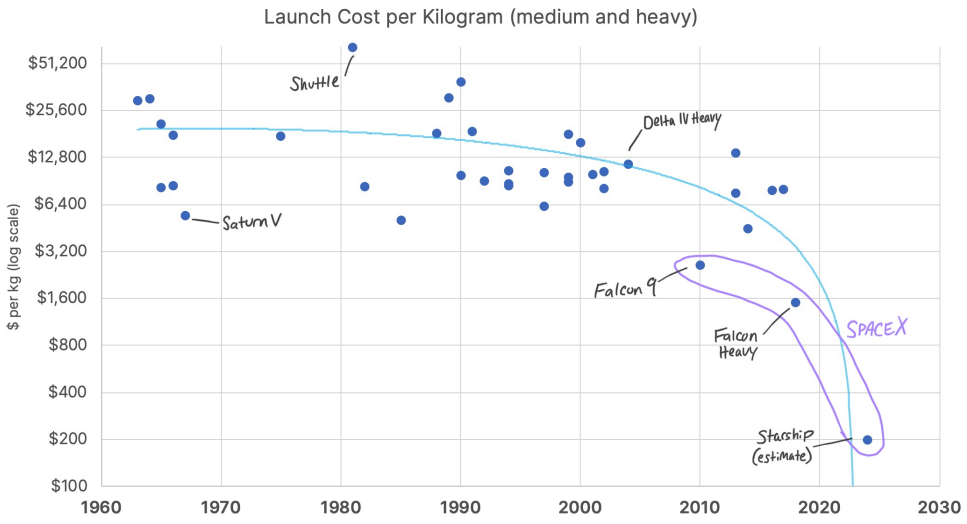


Figure 1.2: Payload launch cost per kilogram. Source [6]

Only in the early 2010s satellite launch costs have been low enough [6] to allow for a substantial number of satellites to be launched in low earth orbit (LEO) orbits, in order to provide adequate coverage area on the Earth surface, together with low latency and larger bandwidth. Figure 1.2 depict this trend.

Complementing the services offered by satellites are high altitute platform (HAP) and unmanned aerial vehicle (UAV), both offering lower deployment costs and times than on-orbit vehicles. UAVs, flying at low altitudes (typically no more than 1km) can guarantee on-demand support for ground networks, providing immediate assistance in instances where regular cell towers are overwhelmed by traffic, or even unusable. HAPs offers a wider coverage area thanks to their higher working altitude (from 20km to 50km), enabling cost-effective wireless coverage to unpopulated areas, together with providing services like backhauling and mobile edge cloud (MEC) capabilities. The assistance offered to the existing network infrastructure by HAP and UAV can play an important role in the public safety scenario, creating an additional communication channel for where an when needed, i.e. during large events. HAPs have shown to be an effective solution both when working as node base (NB) as well as repeater on a bent-pipe architecture [7].

One of the main opportunities offered by 5G is the use of high frequencies, called mmWave spectrum, where higher bandwidth channels can be exploited to obtain high bandwidth and low latency communications. Although the use of mmWaves has been mainly relegated to non-communication services like weather forecasting and TV, due to the high propagation losses caused by high frequencies, recent advancement in this area have allowed the consideration of spaceborne and aerial vehicles that operates at high frequencies. Combined with recent advancements in electronic circuits and antenna designs, this opens the possibility for a NTN to work seamlessly alongside ground infrastructures, creating a viable way of extending system capacity, together with enabling NTN to create high capacity and highly steerable links.

The creation of a flexible tool, able to simulate a multitude of possible combinations in the NTN scenario, is helpful in the identification process that leads to the pinpoint of the viable options that might shape the future of the telecommunications landscape. The option to test novel concepts, protocols and networks configuration on a sandbox environment that eliminates or reduces the need for on-the-field testing facilitate the research process. Furthermore, an open source and freely available simulator offers industries and corporations a way to categorize and evaluate what technologies offers commercially viable opportunities.

Academic and industrial research on creating a network simulator for NTN has been made, 5G K-Simulator [8], and the Matlab based 5G system simulator 5GVienna [9] are viable options, but both requires some type of commercial licenses to use, toghether with Simu5G [10] which also requires commercial license for industrial use. Another possibility

represent 5G-air-simulator [11] that however, while being a free-to-use open source solution, only focuses on the air interface technology.
This thesis aims at creating an open source module for network simulator 3 (NS-3) that implements the NTN channel model, which can serve as a tool in the study of the challenges posed by satellite communications, together with providing objective results in the trade-offs investigation process. The wide simulation spectrum of frequencies available (0.5GHz to 100GHz) together with the ease to expand structure of the implemented code offers research opportunities that spans a variety of cases. The software that act as the starting point of this thesis, NS-3, is an open-source software for full-stack network simulations, offering a high degree of flexibility and extensibility, built with research and teaching purposes in mind.

The implementation process of this thesis is strictly related to the 3GPP recommendations for NTN design, following the proposed procedures and methods, since they offer the state of the art regarding channel modeling, with parameters gathered in simulation campaigns in collaboration with industry leader organizations. All the created code undergoes a resource optimization analysis, being careful to use the appropriate data structures offered by C++ depending on the type of use and the size, staying coherent with the performance optimized NS-3. Furthermore, when a lack of guideline from 3GPP is found on certain matters and details, investigation in latest research findings is done to bring results as updated and as close to reality as possible.

This thesis gives and overview of the 5G structure and channel model, together with highlighting the key aspects of NTN. A presentation of the 3GPP NTN channel model is given, showing the key differences with the terrestrial channel model, and a description of the implementation result is performed. One of the goal is to conduct a simulation campaign, where multiple scenarios are tested, analyzed and discussed, to validate the implementation work.

In particular, the thesis is organized as follow:

- Chapter 2 describes the 5G architecture's achieved and futures goals, and the channel model for 5G is presented.
- Chapter 3 discuss NTN, analyzing their key aspects. The 3GPP NTN channel model is presented highlighting the differences with the 3GPP mmWave channel model.
- Chapter 4 describes the implementation of the NTN channel mode into NS-3, providing a discussion about the changes made to the code and the choices that have been made.
- Chapter 5 presents the simulation scenarios that have been implemented, providing results in order to compare the performance of satellite communication as a function of several parameters and metrics.

- Finally, Chapter 6 concludes the Thesis by drawing some conclusions and shedding light on possible future additions to the presented solutions.

# Chapter 2

# 5G Cellular System

The aim of this chapter is to provide an overview regarding the current state of 5G, together with highlighting some of its key features. Subsequently, the channel model for 5G networks as provided by 3GPP is presented, giving a description of its main aspects.

## 2.1 5G Overview

5G was first formally introduced by 3GPP in 2016, aimed at providing unprecedented amount of services and traffic capability to an ever growing connected society. The deployment of the network is an ongoing process, with phone manufacturers currently offering 5G capable devices, and subscribed users to 5G services in possession of a 5G capable device have reached 690 million subscribers globally in the second trimester of 2022 [1]. Figure 2.1 depicts the global trend in the adoption of 5G services.

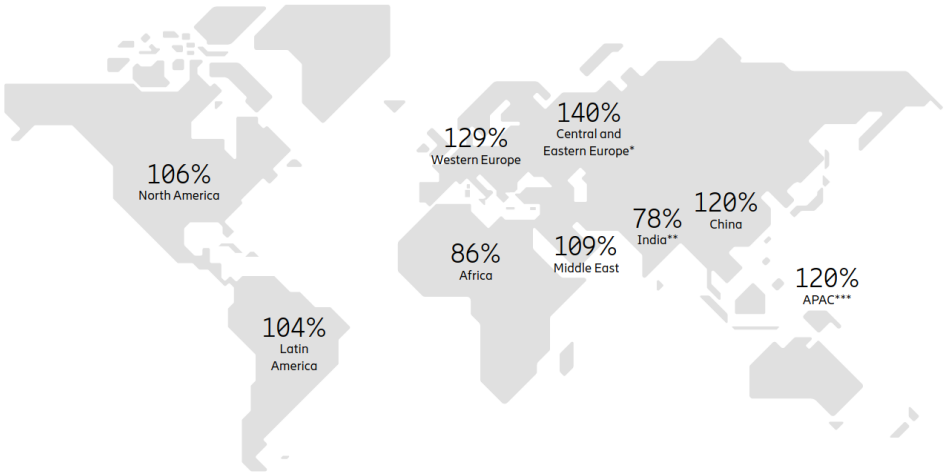


Figure 2.1: 5G subscription penetration during Q2 2022 (percent of population). Image from [2]

While the initial standardization process was finalized in Rel.16 by 3GPP, the evolution is far from complete. For instance, the latest 3GPP Rel.17 discusses satellite access in 5G, while the Rel.18 (scheduled for Q4 2023) will discuss 5G-Advanced. The latter will not be commercially available before 2025, with 5G technologies as a whole expected to provide services up to the next decade at least.

5G, through its multiple development and releases, is expected to offer massive increases in bandwidth capacity, reduced latency times, increased service up-times, and a whole spectra of novel concepts spanning the entire network structure [1]. This chapter aims at giving an overview of 5Gs key concept and enabling technologies, with a focus on the mmWave channel model.

### 2.1.1 Smart infrastructure

5G is being developed with a variety of specificities regarding its capabilities and available services. Multiple novel concepts and technical innovations allow the 5G system to be useful to a new set of markets, being a "vertical" structure. Utilization scenarios include: Critical Communications (CC) and Ultra Reliable and Low Latency Communications (URLLC), massive internet of things (mIoT), automotive and marine communications, discrete automation, electricity distribution, public Safety, health and wellness, etc.

One of the enabling concepts in this regard is network slicing, being the ability of the network operator to dynamically reconfigure the network structure to provide customised levels of functionalities or performance requirements. Network slicing allows the use of the same common hardware equipment by different type of users, offering high network customization capabilities, isolation between the different slices, different performance levels, on-demand scalability and support for multi-vendor and multiple-operator scenarios.

Another example of the adaptability of 5G is the support for multiple radio numerologies, allowing on-request assignment of subcarrier spacing and customized symbol duration, in order to adapt to different latency requirements [12]. The adaptable numerology has shown to improve end-to-end latency and goodput when compared to a fixed numerology approach [13].

The reconfigurable infrastructure of 5G is enabled by a multitude of novel concepts, one of them being network function virtualization (NFV). NFV allows network operators to manage and expand the network capabilities on demand, by implementing certain network functionalities as software applications instead of hardware. This allows for easier load-balancing, up/down scaling and upgrades to functions without service interruption to the user. NFV, as standardized by ETSI [14] virtualizes layer 4 trough layer 7 network functions.

A key enabler to a dynamic infrastructure, working alongside NFV is

software defined networking (SDN). SDN comes into play to overcome the limitations of traditional networks and traditional network operations, by allowing services and applications to reconfigure the network using APIs designed for this specific purpose. SDN centralize network intelligence in one single component, called the Control Plane, which is separated from the data transport process assigned to the Data Plane.

### 2.1.2 New spectrum

With an ever increasing network bandwidth demand, 5G aims at exploiting the enormous amount of spectrum in the millimeter wave (mmWave) bands to greatly increase communication capacity. This new region of the spectrum, which spans roughly from 10 to 300 GHz, brings larger bandwidth opportunities together with multi-gigabit speed capabilities. On the other hand, high frequencies communication introduces a set of challenges that are not present at sub-6GHz frequencies, some of them being the high propagation loss, directivity and sensitivity to blockage.

One of the novel concept introduced with mmWaves, is beamforming antennas. The relative small vawelength of mmWave, together with advances in low-power complementary metal–oxide–semiconductor (CMOS) radio-frequency (RF) circuits enable large numbers of miniaturized antennas to be placed in small dimensions. These multiple antenna systems can be used to form very high gain, electrically steerable arrays. This allows to compensate the high omnidirectional loss introduced at high frequencies [15].

Despite this, the shadowing effect on mmWaves is much greater with respect to lower frequencies: materials such as brick walls can cause attenuation from 40 to 80 dB [16], and even the human body poses a strong attenuation (20-35dB) on the signal strength [17]. Even foliage, water vapour, rain and oxygen are attenuating factors. This reduces the possible range of mmWave communications, placing the cell effective radius limit at approximately 200m [15].

### 2.1.3 Massive MIMO

Beamforming is a signal processing technique, consisting in combining different elements of an antenna array in order to get constructive interference at certain angles, while reducing radiation power on other directions. Beamforming is identified as a key enabler of the 5G infrastructure. This technique however requires the presence of multiple radiating element on the same device or cell tower [18].
As mentioned in the previous section, the short wavelength of mmWave allows for a large number of antennas to be placed in a limited amount of space. The presence of multiple radiating elements in both NB and user equipment (UE) creates multiple spacial channels, from which the name multiple input multiple output (MIMO). MIMO technology have been in

use before the development of mmWaves, but have been limited in the number of used antennas, which where typically in 2x2 or 4x4 configurations (4 and 16 radiating elements, respectively) in the case of 802.11 (2.4GHz and 5GHz Wi-Fi). With 5G not only the number of antennas has been raised, reaching and surpassing 32x32 elements in a single antenna, but have been implemented in UE handheld devices thanks to the smaller size of circuitry required for mmWaves. The high number of radiating elements has led to the "massive" appellation, together with allowing extremely effective beamforming and high spectral efficiency, substantially improving the throughput [19].

## 2.2 5G Channel Model

Standardization bodies (such as 3GPP and IEEE) have worked on creating and keeping up to date documents and tools to properly model and evaluate the performance of 5G mmWaves. Multiple channel models have been presented to support above 6GHz simulations [20] [21] [22]. The work presented in [23], a detailed channel model for mmWaves, is the one considered for this thesis, with the spacial channel model implementation described in [24]. With Release 16 TR 38.901 [25] 3GPP has put together research findings on the channel model for frequencies between 0.5 and 100 GHz, thus including legacy frequencies and mmWaves. This section aims at giving a description of the main components that are presented by [25], since this the latter is the basis for the definition of the NTN channel model.

### 2.2.1 Scenarios and Channel Condition

The environment that is being considered during any simulation, performance evaluation or modeling of a real world use case is crucial in the type of outcome that will be presented. A multitude of parameters changes depending on the position of the UE, NB and surrounding buildings and structures. In this context, 3GPP considers multiple *scenarios*, which are summarized in table 5.2.

Another important variable to get a correct estimate of the channel is the line of sight (LOS) condition. LOS is achieved whenever transmitter and receiver nodes are visible to each other, meaning that the signal can reach the receiver without the need of reflections or material penetration. The opposite of the LOS condition is the not line of sight (NLOS).
Whether the channel is in LOS condition or not, is determined by a probability function that changes with the scenario, and is related to the distance between UE and NB.

| Scenario | Description |
|---|---|
| UMi | Urban scenario (street canyon) with BS antennas located below the roof of buildings |
| UMa | Urban scenario with BS antennas located above the rooftops of the surrounding buildings |
| Indoor Office | Indoor rooms with BS antennas located on the ceiling |
| RMa | Rural deployment focused on larger and continuous coverage. |
| Indoor Factory InF | Factory halls of varying sizes and with varying levels of density of machinery, assembly lines, storage shelves, etc. |

Table 2.1: Different scenarios defined by 3GPP

### 2.2.2 Free-space path loss

The free-space path loss is an always present element in wireless communication system, introducing signal's power degradation. If we suppose ideal conditions, and only free-space path loss as a factor of signal attenuation, we can get the received power at a certain receiving antenna with *Friis law*:

$$\frac{P_r}{P_t} = G_t G_r \left(\frac{\lambda}{4\pi d}\right)^2 \tag{2.1}$$

In 2.1, $P_r$ and $P_t$ are receiver and transmitters powers, $G_t$ and $G_r$ are receiver and transmitters antennas gains, $\lambda$ is the wavelength and $d$ the distance between the endpoints.
The gain of a generic antenna, is described by:

$$G = \frac{4\pi}{\lambda^2} A_{eff} \tag{2.2}$$

Where $A_{eff}$ is the *effective area* of the antenna. From 2.1 and 2.2 we can capture how the propagation loss in free space is greater with increasing frequencies but counterbalanced by the additional antenna gain, since the latest also increases with frequency, thus showing that using higher frequencies does not introduce inherited disadvantage in terms of free space path loss.
If isotropic antennas of unitary gain are supposed, and we brings the equation into the logarithm domain, a more general formula would be:

$$FSPL_{dB} = A + Blog_{10}d + Clog_{10}f \tag{2.3}$$

Where $A$ and $B$ are parameters that changes depending on the scenario from table 5.2, $d$ is the distance and $f$ is the transmitting frequency. More specifically, $B$ accounts for the dependence on the distance between receiver and transmitter, $C$ dictate the relationship to the carrier frequency and $A$ get assigned different values depending on the scenario

and LOS/NLOS condition. An additional value called break point distance $d_{BP}$, determined by the frequency together with the heights of the NB and UE, is necessary to determine the correct value of $FSPL_{dB}$. Equation 2.3 is the first step in the calculation of the link budget in the 3GPP model.

### 2.2.3 Atmospheric absorption

Due to the nature of air and water vapour molecules, whose tends to absorb the energy of an electromagnetic wave which wavelength is similar to their size, stronger attenuation can affect the signal at certain wavelengths. This effect is present in considerable magnitude only at specific frequencies, reaching values of tens of dBs around two main peaks: one around 60GHz (for resonance with oxygen molecules) and the other at 180GHz (for water vapour absorption) [26], as illustrated in figure 2.2.

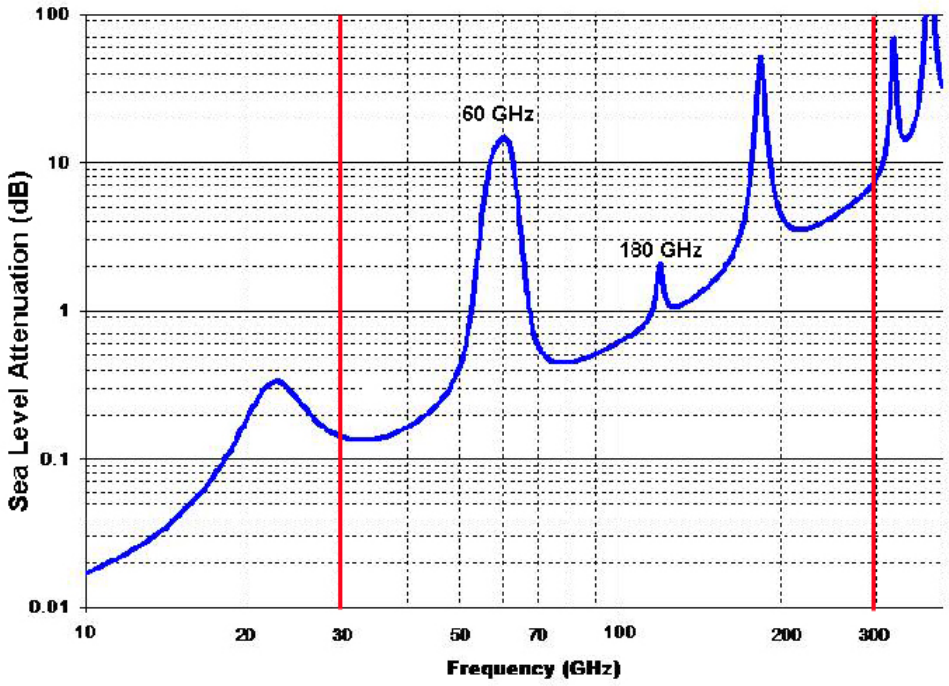


Figure 2.2: Water Vapour and Dry Air attenuation at sea level, from [27]

The attenuation varies with humidity percentage, barometric pressure and altitude from the sea level. A proper selection of the frequency bands is required to avoid these high attenuation wavelengths, and most transmission band in use have been chosen to avoid these effects.
The considered implementation of the spacial channel [24] does not implicitly model this effects, while 3GPP gives a calculation process in case of *advanced simulations*, listing some cases where a simulation scenario might be considered so: presence of very large arrays and large band-

width, transmission frequencies between 53 and 67 GHZ, large number of closely located user, etc.

### 2.2.4 Shadowing

Shadowing is the effect experienced by the signal due to objects in the propagation path. The multiple versions of the signal arrives at the receiver, each one experiencing a different path and thus bringing a different amplitude and phase shift, together with different delays. This can result in either constructive or destructive interference, and make the power of the received signal fluctuate over time, as can be seen in figure 2.3.

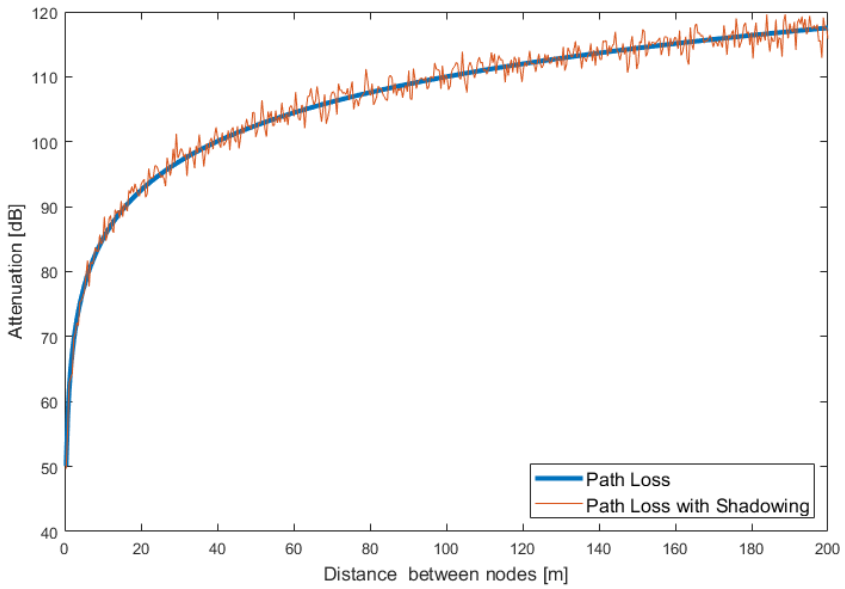


Figure 2.3: Path loss compared to path loss with shadowing

Shadowing is modeled as a log-normal random variable of mean zero and standard deviation $\sigma$, dictated by the scenario and the LOS condition.

### 2.2.5 Coordinate System

3GPP uses a Cartesian coordinate system where the position of each node is uniquely described by three values $(x, y, z)$, with $x$ and $y$ spanning the ground plane, and $z$ indicating the height of a certain node. This positioning system is adequate to represent the position of each UE and NB, but when considering arrival and departure angles at a specific antenna a different set of coordinates is implemented, which is composed of spherical coordinates. A generic point in spherical coordinates is described as $(r, \phi, \theta)$, but since the operations performed with these sets of

coordinates concerns antenna field patterns, the radial component $r$ is dropped, leaving the *inclination* $\theta$ and *azimut* $\phi$.

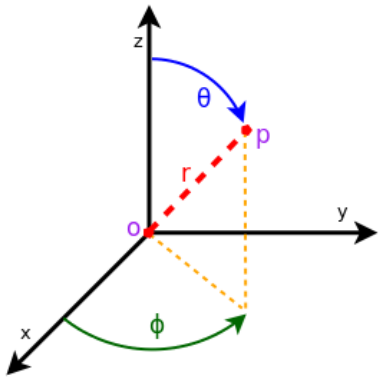


Figure 2.4: Polar coordinate system (LCS)

In the 3GPP TR [25] the Cartesian coordinates takes the name of global coordinate system (GCS), while the polar coordinates are named local coordinate system (LCS). A proper method of translation between the two system is required when using antenna's field patterns, and [25] describes the translation process currently implemented into the mmWave module of NS-3.

### 2.2.6 Antenna models

Antennas described by [24] are modeled as phased arrays, meaning that an antenna of either a NB or UE is composed of multiple elements. This type of antennas are also called uniform planar arrays (UPA), and are widely used when dealing with high frequencies, thanks to the offered beamforming capabilities. Each antenna contains $N_{a,c} \times N_{a,r}$ elements, with $r$ being the number of rows and $c$ the number of columns. The elements of an antenna are equally spaced, and the antenna orientation can be configured by adjusting bearing, tilt and slant angles. The current implementation suppose a fixed slant angle equal to 0.
Since the 3GPP standard specifies the antenna field pattern as a function of zenith and azimuth angles of arrivals $(\theta, \phi)$ with $(\theta \in [0°, 180°], \phi \in [-180°, 180°])$, the global coordinates needs to be translated into the local coordinates of the antenna. Having these values, the radiation power pattern of an UPA is defined as follow:

$$A_{dB}(\theta, \phi = 0°) = -min\left\{12\left(\frac{\theta - 90°}{\theta_{3dB}}\right)^2, SLA_v\right\} \tag{2.4}$$

$$A_{dB}(\theta = 90°, \phi) = -min\left\{12\left(\frac{\phi}{\phi_{3dB}}\right)^2, A_{max}\right\} \tag{2.5}$$

With $\theta_{3dB} = \phi_{3dB} = 65°$ and $SLA_v = A_{max} = 30dB$. Combining 2.4 and 2.5 gets the 3D radiation power pattern:

$$A_{dB}(\theta, \phi) = G_{E,max} - min\left\{-\left(A_{dB}(\theta, \phi = 0°) + A_{dB}(\theta = 90°, \phi)\right), A_{max}\right\} \tag{2.6}$$

Where $G_{E,max}$ is the maximum gain of the antenna, which upper limit is set to $8dBi$.
The antenna array model as implemented in [24] support the assignment of a beamforming vector to each antenna, while the beamforming algorithm choice is arbitrary.

### 2.2.7 Channel Matrix

3GPP models the channel using a channel matrix. Each combination of UE and BS calls for the calculation of a separate channel matrix. The channel matrix $\mathbf{H}(t, \tau)$ is a $U \times S$ matrix, where $U$ and $S$ are the number of antennas at the receiver and at the transmitter, respectively. Each entry of the matrix depends on $N$ different multipath components, called *clusters*, and each component has different delay and received power. Both received power and delay are dictated by an exponential profile. Each cluster includes multiple *rays*, and all the rays in a cluster experience the same power profile and propagation delay, together with similar angles of arrival $\left(\theta^A_{n,m}, \phi^A_{n,m}\right)$ and departure$\left(\theta^D_{n,m}, \phi^D_{n,m}\right)$. All of these parameters are drawn from the technical report, and vary according to the scenario and channel conditions.
Fading components can be divided into two:

- Large scale parameters, which include delay spread, angle of arrival and departures, etc. that depends on user mobility or changes in the scenario.
- Small scale parameters, such as the delay of the different clusters, the arrival and departure angles of the rays, the variation in the power of the different clusters, etc. which depends on the small variations of the multipath components.

The channel matrix calculation is broken down into a list of steps. The first 3 steps deal with propagation loss. Step number 4 relies on the pre-computed correlation matrices, and consist in the generation of the large scale parameters. Step 5 and 6 take care of the cluster delays and powers. The seventh step generates arrival and departure angles, and in a LOS case a Ricean factor $K$ is added. Step 8 and 9 performs rays coupling and create cross polarization powers, respectively, with step 10 consisting in drawing the initial random phases from a uniform distribution. The last step, number 11, consist in the final generation of the complete channel matrix

# Chapter 3

# Non-Terrestrial Networks

A NTN, from a wide prospective, is any network that include flying objects. The NTN terms include satellite communication networks, HAP and UAV, and any air-to-ground network. Satellite communication networks include LEO, medium earth orbit (MEO) and GEO satellites.
NTN are recognized by researchers as a key component in the future of wireless communications, including but not limited to, the 5G development process. Work by 3GPP on NTN started in 2017 with Rel-15 [28], with the objective of selecting reference deployment scenarios. After that, Rel-16 and Rel-17 have advanced the work adding the possible impact on the NR structure.

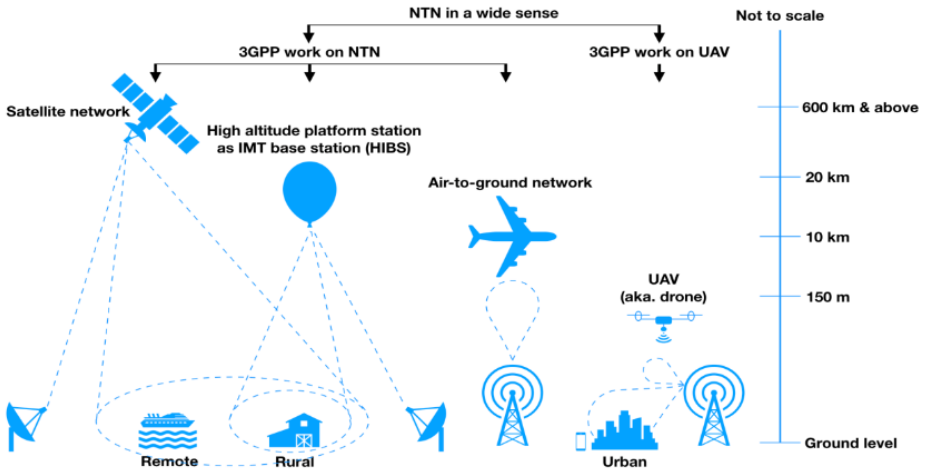


Figure 3.1: NTN types of scenarios. Picture from [29]

This chapter is a description of the possibilities offered by NTNs, together with the challenges introduced by these type of networks. Then, a description of the 3GPP channel model for NTN is given, highlighting the difference with the mmWave channel model presented in [25].

## 3.1 NTN Overview

### 3.1.1 NTN use cases

Current services provided by satellite includes, but are not limited to, navigation, meteorology, television broadcasting and remote sensing. Combining aerial infrastructure with terrestrial ones opens a whole new set of possible use cases. This section aims at identifying some possible improvement that a non-ground based network can provide to the existing infrastructure, together with new type of services.

#### Service Continuity

NTN stations can provide an additional backup connection where ground station might be temporarily unavailable. In the case of natural disasters or other emergency situations the ground infrastructure might not be enough to ensure connectivity, or even being damaged, and NTN can provide wireless coverage ensuring communication between emergency services.

#### Load Balancing

When a hot-spot area is created, with a large number of users served by a small number of cell towers, the existing infrastructure might get overloaded. The support of spaceborne/aerial vehicles would increment the possible number of connected users in the same area, ensuring service continuity even during exceptional events where a large gathering of people is present, such as sports matches, evacuations, and so on.

#### Service Ubiquity

The nature of spaceborne and aerial vehicle provides high area of coverage on the ground, with footprint sizes going from 5km for UAV to 3500km offered by GEO orbits [30]. This make possible for NTN to provide services even where normal ground infrastructure would not be practically feasible to build, including unpopulated areas or remote locations.

#### IoT and MTC

One of the objectives of 5G is to serve as a communication structure not only for users, but also for sensors, machinery, unmaned vehicles, etc. mIoT and machine type communications (MTC) might require connection where normal communication infrastructure is not present. NTNs can provide connectivity to devices located in areas where human presence is not regular, enabling data gathering where it would otherwise be unfeasible.

#### Mobility

Providing connectivity to in-motion terminals, especially fast moving like vessels or planes, requires to frequently perform handovers. Thanks to high coverage area, toghether with inter-satellite link (ISL), NTNs can help alleviate these limitations of ground based infrastructures.

#### Global Satellite Overlay

When the distance between two ground nodes increases, the amount of network devices which are involved in the communication by the two entities might get preferable to opt for a satellite link, where inter-satellite connections comes into play to create an overlay mesh network. This will reduce the load on the ground network, routing the information throughout the satellite only network to the destination node.

### 3.1.2 NTN platforms

When rockets launch satellites, they put them into an orbit. The type of orbit chosen for a satellite is crucial in dictating what type of services the spaceborne vehicle will provide. We can identify a series of parameters, useful for telecommunications purposes, that are being set by the type of orbit selected:

- Ground footprint, being the extension of the ground area at wich the satellite can provide services to.
- Distance from the ground. Higher distances cause higher communication delay, and more severe propagation losses.
- Orbital velocity or orbital period, which is related to how much time it takes for the satellite to complete one revolution of its orbit.
- Elevation angle, described as the angle from the ground plane where the observer is located to the vector pointing at the satellite. This parameter clearly changes over time even for the same space vehicle, if the latter is moving with respect to the ground.

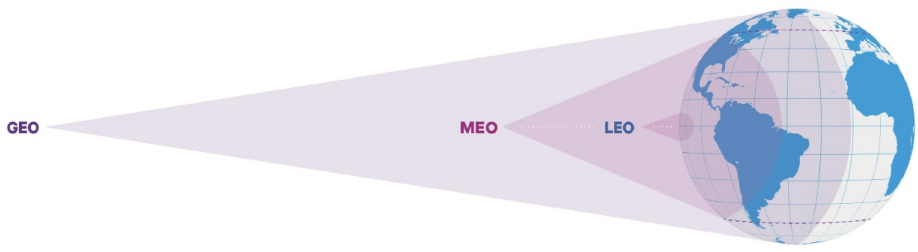


Figure 3.2: Different orbits and their coverage area

The following section gives an overview of the main advantages and downsides of a certain orbit type. The orbits type presented are coherent with the ones being considered by 3GPP in [28], meaning that other type orbit exists, but are not considered relevant in the NTN scenario as of now.

### GEO

As the name suggest, these type of orbits offers a main advantage: the satellite always covers the same area on the ground, with an orbit time of 23 hours 56 minutes and 4 seconds and travelling at roughly 3km per second. An first implication of this is that ground terminals can always rely on finding the same spaceborne vehicle serving them. Secondly, given their great altitude of 35786km from the Earth's ground they cover an extensive surface. The immediate drawback that comes from their great distance from Earth is longer propagation delays, together with high signal attenuation due to pathloss.
Being this far away from the Earth atmosphere, GEO experience low level of drag and have a longer lifespan compared to satellite placed on lower orbits.
Historically, this orbits has hosted weather, TV broadcast and low speed communication satellites.

### LEO

Low Earth Orbit places satellites at an altitude of less than 1000 km, but could be as low as 160 km. Unlike GEO's satellite, LEO's can have a *tilted* orbit, meaning that their trajectory does not need to follow the equatorial line.
At this altitude, the orbital velocity is roughly 7.4km per second, taking approximately 90 minutes to complete a full revolution around the Earth. The ground footprint size is upper limited to 1000km, meaning that a large number of satellites are needed to cover entire countries or continents. This problem is marginally alleviated by the reduced cost of launch compared to GEO satellites. It is the orbit most commonly used for satellite imaging, as being near the surface allows it to take images at higher resolution.
Individual LEO satellite pose more critical constraints as long as communication is concerned, since they travel so fastin space that the available communication windows tends to be short, in the order of some tens of minutes. This is why when building communication networks using the LEO orbit *constellations* of satellites are typically considered, where multiple satellite are coordinated to in sync and route information between each other using the support of ground stations or ISL.
Recently, large satellite constellation (e.g., Starlink, Kuiper, and OneWeb) have been deployed in this orbit to offer high bandwidth and low latency internet connectivity.

The drag level given by the atmosphere is highly relevant, making the lifespan of LEO's spaceborne vehicles between 7 and 10 years [31].

#### MEO

Satellites in MEO orbits have an altitude between 2,000 and 35,786 km, and a minimum rotational period of 2 hours, that can extend up to 24 hours. MEO have been extensively used for navigation constellations, such as GPS, GLONASS, Galileo, etc. The 3GPP definition of MEO is more strict in terms of altitude, restricting the range from 7000km to 25000km [30].
The footprint size of a satellite in this orbit is included from the one offered by LEO's satellites up to the one achieved by GEO's ones, as are time delay values and attenuation from pathloss.

#### Aerial Vehicles

Vehicles in these category are not satellites and do not follow a precise orbit, but are included since they are one key NTN technology according to the 3GPP. Aerial vehicles are divided into UAV and HAP. HAP is a station located on an aerial object at an altitude from 20 to 50 km and at a specified, nominal, fixed point relative to the Earth, while UAV are flying drone-like vehicles reaching a mimum altitude of 1km. The footprint size of these category is reduced to some tens of km for UAV and between 300km to 400km for HAP.
Typical application scenarios for UAV and HAP are high bandwidth connectivity to a relative small area on the ground, where ordinary communication infrastructures are experiencing overload and down times.
While areal vehicles clearly offers many opportunities for NTNs, this thesis is more focused on satellite scenarios.

### 3.1.3 NTN challenges

Despite offering multiple improvements, NTN is still a novel concept, that brings a lot of open challenges. The correct identification and classification of these matters is essential in addressing them, and in advancing the research towards the deployment of NTN. This section gives a brief overview of the open issues that needs further investigation, which are discussed in detail in [32] and [33].

#### Doppler effect

LEO satellites are typically high-velocity vehicles, and their relative speed to the receiving or transmitting equipment introduces high values of Doppler shift. Existing devices might not be equipped with the proper tool to manage the frequency shifts of these magnitudes, and need software or hardware adaptations.

#### Propagation Delay

High propagation distances implies high propagation delays. This might have repercussions on the existing protocol stack. Namely, the extremely widely used Transmission Control Protocol (TCP) might have problems coping with high Round Trip Times (RTT) and low bandwidth availability of channels of certain NTN scenarios, such as GEO orbits. Work on delay-tolerant network [34] and the use of compatibility layers can help mitigate these problem.

#### HARQ

Hybrid Automatic Repeat reQuest (HARQ) operations are time-critical operations. In satellite communication, the RTT normally exceeds the maximum conventional HARQ timers and the maximum possible number of HARQ processes. Even in LEO constellations, the RTT can be between 15 to 63 times higher than that of a terrestrial network [28]. Memory restrictions in certain UEs devices might make it unfeasible to simply extend HARQ timers, making research on this matter a crucial.

#### Coexistence

NTN are considered an additional part of the existing 5G infrastructure, and not a replacement. Additional interference might be created, even in vast areas, by spaceborne and flying telecommunications nodes. This might cause existing ground networks, especially if already on the limit of acceptable noise levels, to stop working properly.
Studies by 3GPP on this matter are an open topic, with on going research being made.

## 3.2 NTN Channel Model

Enabling 5G systems to support NTNs has been one direction under exploration by the 3GPP. In this regard, proper channel modelling is crucial in the identification of the possible deployment scenarios. The latest channel model for NTNs has been documented by 3GPP with TR 38.811 [28]. This section is centered on presenting the NTN channel model, highlighting key differences with the channel model for regular ground networks presented in [25].

### 3.2.1 Differences with the cellular channel model

While differences between the NTN and cellular channel models on specific matters will be treated singularly in the following sections, and overview on the grand-scheme and immediate distinctions is needed.
LEO satellites speed taking as reference a ground observer, is changing

over time, reaching its peak while crossing the 90 degrees of elevation angle. This introduces a *dynamic delay*, being the delay between receiver and transmitter that does not remain constant in time.
Related to satellite mobility, is the Doppler shift caused by the high differential velocity that might be present in NTNs, especially when deployment scenarios include LEO and MEO orbits. Figure 3.3 gives a visual representation of the main differences between terrestrial and satellite channel. Scintillation and other effects that the atmosphere induce on the signal will be analyzed into dedicated sections.

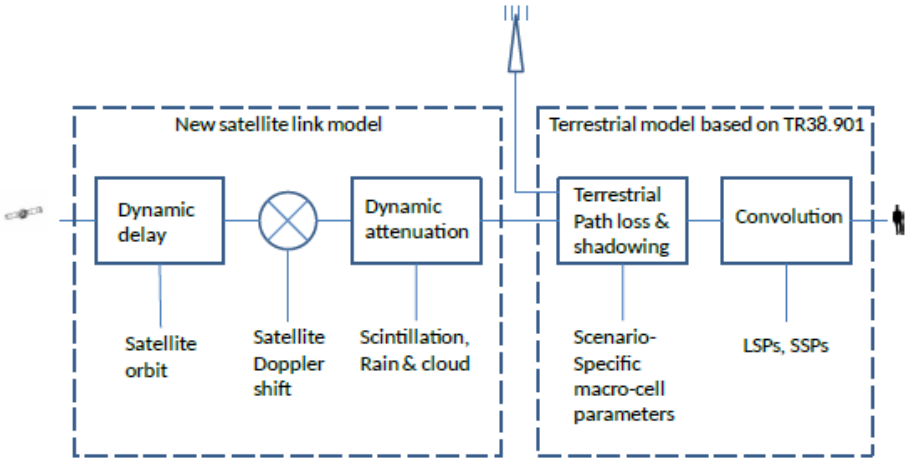


Figure 3.3: Conceptual drawing of satellite and terrestrial channels, from [28]

### Angular Spread

The receiver typically does not obtain one single version of the transmitted signal, but multiple signals with different angles of arrivals are collected due to multipath propagation. Multipath propagation is due to reflection and diffraction of the signal along its path. This effect is modelled in a value called angular spread, represented as normal random variable of given mean and variance, which depends on the deployment scenario.
Due to the distant location of satellites, the angular spread of multipath propagation is almost zero, hence the received signals components are either parallel with the main propagation path or tangent to it, as depicted in figure 3.4. This holds true in the case of LOS, while in the case of NLOS condition the spread can be compared to the one present in terrestrial cellular networks, since the signal power is mainly given by reflections of the main signal component.

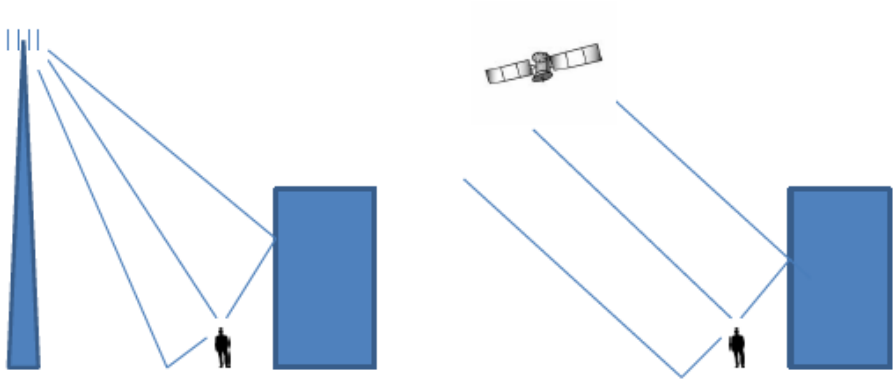

Figure 3.4: Angular spread comparison between a ground based NB and a satellite NB, from [28]

#### Frequency Bands

Even if the technical report keeps into consideration the spectrum of frequencies from 0.5 to 100GHz, 3GPP identifies two main bands of interest for the NTN channel [30][28]. The first is the S band, centered at around 2GHz and with 20MHz wide channels, one for down link (DL) and one for up link (UL). The second band of interest is the Ka (*"K-above"*) band, which positions the UL frequency at 20GHz and the DL one at 30GHz. Table 3.1 summarizes the outline for the frequencies of interest.

| | **UL** | **DL** | **Bandwidth** |
|---|---|---|---|
| **S band** | 1980 - 2010 MHz | 2170 - 2200 MHz | Up to 2*20 MHz |
| **Ka band** | 29.5 - 30 GHz | 19.7 - 21.2 GHz | Up to 2*800 MHz |

Table 3.1: Frequency bands of interest for NTN

### 3.2.2 Coordinate System

Traditional coordinates system used by 3GPP positions the nodes in 3D space using a set of three variables, forming a *Cartesian plane*, that will be described in chapter 4. This has a strong implication: the Earth's ground is modeled as flat. The latter simplification is justified when only considering ground placed structures, with cell towers and users located no more than some hundreds of meters apart, but makes this positioning system unusable for NTN scenarios where the Earth spherical shape has high relevance.
Related to this, 3GPP has suggested a new coordinates system, namely the *Geocentric Cartesian* coordinate system, also called Earth centered Earth fixed (ECEF). A UE or satellite position is described by a set of three parameters $(x, y, z)$, and the Earth is approximated as a true sphere with radius of 6371km. The origin of the coordinate system is located

at the center of the Earth, and the $x - y$ plane lies on the equatorial plane, with the $x$ axis pointing the 0 degree longitude and the $y$ axis pointing the 90 degree longitude. The $z$ axis point to the north pole, with origin in the Earth's center. The use of this coordinate system is also necessary for the calculation of the *elevation angle*, a central value for the NTN channel, as it will used multiple times to obtain various parameters. A recommendation on a condition to be met is made in the 3GPP document, to respect a level of coherence with the real world: $\sqrt{x^2 + y^2 + z^2} = 6371km$ for all UEs and $\sqrt{x^2 + y^2 + z^2} > 6371km$ for all satellites.

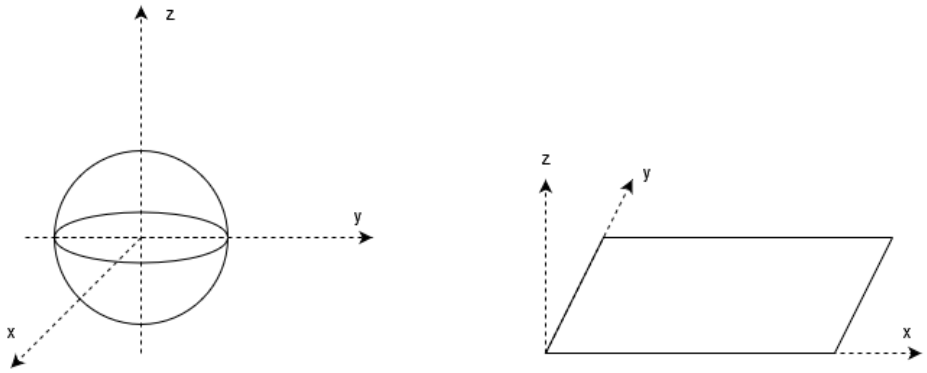


Figure 3.5: Geocentric Cartesian or Earth Centered Earth Fixed coordinates, compared to planar Cartesian coordinates

### 3.2.3 Scenarios and Channel Condition

#### Scenarios

Similarly to what concerns the ground channel model and presented in section 2.2.1, the NTN model gives the option to place the simulation environment in four different *scenarios*, that determine a magnitude of propagation characteristics. Only outdoors conditions are considered for satellite use cases, where the attenuation given by being inside a building would be enough to make the signal unusable. For HAPs instead, indoor conditions are possible.
Scenarios differs in the density of signal blocking elements, such as buildings, trees and natural structures. Table 3.2 gives a description for each scenario.

#### Line Of Sight condition

The probability for a ground terminal of being in LOS condition with a satellite, is determined by two parameters: scenario and elevation angle. The scenario of reference is a choice made beforehand, while the elevation angle is a parameter determined by the node's positions. The elevation

| | **Circular Aperture** |
|---|---|
| **Dense Urban** | Extremely building-dense enviroment, with high buildings |
| **Urban** | City enviroment, but medium to high density presence of buildings |
| **Suburban** | Small cities, with maximum two storey buildings |
| **Rural** | Little or no presence of buildings, open fields |

Table 3.2: Possible scenarios for NTN channels

angle is defined as the angle between the horizon plane of the ground terminal and the vector pointing to the satellite.

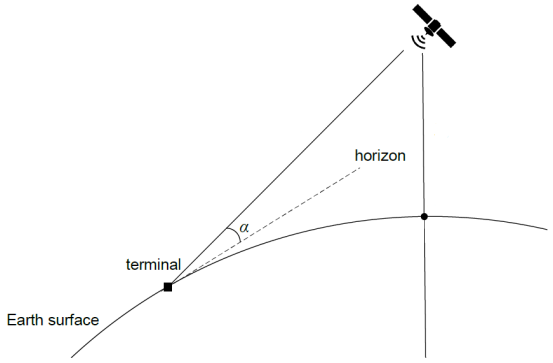


Figure 3.6: Depiction of the elevation angle $\alpha$

For the NTN channel model 3GPP provides the LOS probabilities on a chart (reported in Table 3.3), where knowing the scenario and elevation angle return a percentage value. This is a key difference from the regular channel model, where the LOS probability calculation need the scenario, together with distance between the nodes with their respective heights.

| Elevation | Dense urban | Urban | Suburban and Rural |
|---|---|---|---|
| **10°** | 28.2% | 24.6% | 78.2% |
| **20°** | 33.1% | 38.6% | 86.9% |
| **30°** | 39.8% | 49.3% | 91.9% |
| **40°** | 46.8% | 61.3% | 92.9% |
| **50°** | 53.7% | 72.6% | 93.5% |
| **60°** | 61.2% | 80.5% | 94.0% |
| **70°** | 73.8% | 91.9% | 94.9% |
| **80°** | 82.0% | 96.8% | 95.2% |
| **90°** | 98.1% | 99.2% | 99.8% |

Table 3.3: Probability of being in LOS condition, for each scenario

### 3.2.4 Path Loss

The basic path loss (in dB) is composed as follow:

$$PL_b = FSPL(d, f_c) + SF + CL(\alpha, f_c) \tag{3.1}$$

The first term is the free space path loss $FSPL(d, f_c)$, which can be calculated as:

$$FSPL(d, f_c) = 32.45 + 20log_{10}(f_c) + 20log_{10}(d) \tag{3.2}$$

Where $f_c$ is the carrier frequency in GHz and $d$ is the distance in meters between the nodes.
$SF$ represents shadow fading (SF) and is modeled as a log-normal random variable of mean zero and variance $\sigma_{SF}$, i.e., $SF \sim N(0, \sigma_{SF}^2)$. In order to calculate the SF variance, four values are needed: the scenario, the frequency band, the LOS condition and the elevation angle. These parameters are used to find the correct entry on a table, provided in [28] A similar process is needed to calculate the clutter loss $CL(\alpha, f_c)$, but here the reference table directly provides the attenuation value in dB, since this effect is not modeled as a random process. All the values for SF and CL are present in table 3.4, table 3.5 and table 3.6.

| Elevation | S-band | | | Ka-band | | |
|---|---|---|---|---|---|---|
| | LOS | NLOS | | LOS | NLOS | |
| | $\sigma_{SF}$ (dB) | $\sigma_{SF}$ (dB) | CL (dB) | $\sigma_{SF}$ (dB) | $\sigma_{SF}$ (dB) | CL (dB) |
| 10° | 3.5 | 15.5 | 34.3 | 2.9 | 17.1 | 44.3 |
| 20° | 3.4 | 13.9 | 30.9 | 2.4 | 17.1 | 39.9 |
| 30° | 2.9 | 12.4 | 29.0 | 2.7 | 15.6 | 37.5 |
| 40° | 3.0 | 11.7 | 27.7 | 2.4 | 14.6 | 35.8 |
| 50° | 3.1 | 10.6 | 26.8 | 2.4 | 14.2 | 34.6 |
| 60° | 2.7 | 10.5 | 26.2 | 2.7 | 12.6 | 33.8 |
| 70° | 2.5 | 10.1 | 25.8 | 2.6 | 12.1 | 33.3 |
| 80° | 2.3 | 9.2 | 25.5 | 2.8 | 12.3 | 33.0 |
| 90° | 1.2 | 9.2 | 25.5 | 0.6 | 12.3 | 32.9 |

Table 3.4: Shadow fading and clutter loss for dense urban scenario

| Elevation | S-band | | | Ka-band | | |
|---|---|---|---|---|---|---|
| | LOS | NLOS | | LOS | NLOS | |
| | $\sigma_{SF}$ (dB) | $\sigma_{SF}$ (dB) | CL (dB) | $\sigma_{SF}$ (dB) | $\sigma_{SF}$ (dB) | CL (dB) |
| 10° | 4 | 6 | 34.3 | 4 | 6 | 44.3 |
| 20° | 4 | 6 | 30.9 | 4 | 6 | 39.9 |
| 30° | 4 | 6 | 29.0 | 4 | 6 | 37.5 |
| 40° | 4 | 6 | 27.7 | 4 | 6 | 35.8 |
| 50° | 4 | 6 | 26.8 | 4 | 6 | 34.6 |
| 60° | 4 | 6 | 26.2 | 4 | 6 | 33.8 |
| 70° | 4 | 6 | 25.8 | 4 | 6 | 33.3 |
| 80° | 4 | 6 | 25.5 | 4 | 6 | 33.0 |
| 90° | 4 | 6 | 25.5 | 4 | 6 | 32.9 |

Table 3.5: Shadow fading and clutter loss for dense urban scenario

| Elevation | S-band | | | Ka-band | | |
|---|---|---|---|---|---|---|
| | LOS | NLOS | | LOS | NLOS | |
| | $\sigma_{SF}$ (dB) | $\sigma_{SF}$ (dB) | CL (dB) | $\sigma_{SF}$ (dB) | $\sigma_{SF}$ (dB) | CL (dB) |
| 10° | 1.79 | 8.93 | 19.52 | 1.9 | 10.7 | 29.5 |
| 20° | 1.14 | 9.08 | 18.17 | 1.6 | 10.0 | 24.6 |
| 30° | 1.14 | 8.78 | 18.42 | 1.9 | 11.2 | 21.9 |
| 40° | 0.92 | 10.25 | 18.28 | 2.3 | 11.6 | 20.0 |
| 50° | 1.42 | 10.56 | 18.63 | 2.7 | 11.8 | 18.7 |
| 60° | 1.56 | 10.74 | 17.68 | 3.1 | 10.8 | 17.8 |
| 70° | 0.85 | 10.17 | 16.50 | 3.0 | 10.8 | 17.2 |
| 80° | 0.72 | 11.52 | 16.30 | 3.6 | 10.8 | 16.9 |
| 90° | 0.72 | 11.52 | 16.30 | 0.4 | 10.8 | 16.8 |

Table 3.6: Shadow fading and clutter loss for dense urban scenario

### 3.2.5 Atmospheric absorption

Attenuation induced by the presence of atmospheric gasses was a marginal factor in the terrestrial channel model, being left to calculation only in peculiar simulation, as mentioned in chapter 2 section 2.2.3. This is not the case for the NTN channel, where this type of attenuation plays a more relevant role in the final outcome, thus considering it is crucial. A complete and accurate calculation on this effect requires a set of parameters not usually available during simulations, such as absolute humidity, dry air pressure, water-vapour density and water-vapour partial pressure. This precise estimate process is presented in the ITU-R P.676 document [27].
3GPP offers a simplified method, based on the original method by ITU, considering only UEs placed at sea level and setting all the required parameters to their mean annual global values. Fixing the elevation angle at 90 degrees (zenith), the following attenuation values are obtained (figure 3.7), for frequencies between 0 and 350 GHz.

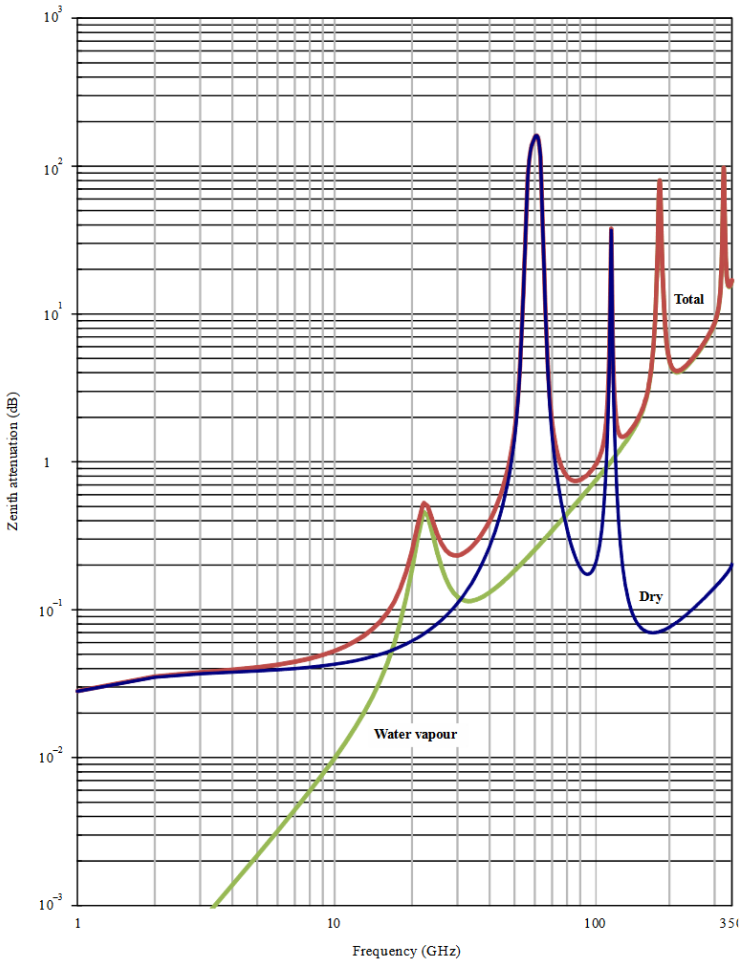


Figure 3.7: Atmospheric absorption values at the sea level, with zenith elevation angle. Graph from [27]

For elevation angles different than 90 degrees, the calculation is straightforward. Given the zenith attenuation $A_{zenith}(f_c)$, the path loss due to atmospheric gasses is:

$$PL_{A,dB}(\alpha, f_c) = \frac{A_{zenith}(f_c)}{sin(\alpha)} \tag{3.3}$$

Where $\alpha$ is the elevation angle in consideration. The loss due to atmospheric absorption should be considered only for frequencies above 10GHz, or for any frequency in the case of elevation angle of less than 10 degrees.

### 3.2.6 Scintillation

Scintillation corresponds to the rapid fluctuation in amplitude and phase of the received signal, caused by the variation of the refractive index of the propagation medium. This phenomenon can be divided into two: ionospheric scintillation and tropospheric scintillation.
Scintillation depends on location, time of the day, season, solar and geomagnetic activity. Stronger levels of scintillation are observed only at high latitude locations (more than 60 degrees), in auroral and polar regions. Similarly to how atmospheric absorption is treated, a simplified model is recommended by 3GPP, since a complete scintillation model would be unfeasible, not to say unnecessary, for system level simulations. The following section presents the two recommended model for ionospheric and tropospheric scintillation.

#### Ionospheric Scintillation

This proposed method for the ionospheric scintillation loss is based on the *Gigahertz scintillation model* [35]. This model is limited to low and medium altitudes (less than 60 degrees). Additionally, scintillation between 60 and 20 degrees of latitude can be considered zero for the purpose of system level simulations, together with also being irrelevant for frequencies above 6GHz. The final formula for calculating losses due to ionospheric scintillation is:

$$PL_{S,dB} = \left(\frac{f_c}{4}\right)^{-1.5} \frac{P_{fluc}(4GHz)}{\sqrt{2}} \tag{3.4}$$

Where $f_c$ is the frequency of interest, and $P_{fluc}(4GHz)$ is equal to the ionospheric attenuation level at 99% of time between March 1977 and March 1978 measured in Hong Kong at 4GHz of frequency, equal to 1.1.

#### Tropospheric Scintillation

Unlike ionospheric scintillation the effect of tropospheric scintillation increases with frequency, and becomes significant above 10 GHz. Again,

3GPP recommends considering the path loss induced by this effect only in certain cases, and offers a direct method for calculation. For any simulation with carrier frequency above 6GHz, the path loss due to tropospheric scintillation is the attenuation measured in Tolouse with 99% probability at 20GHz. Furthermore, a dependency on the elevation angle is introduced, with higher elevation angles requiring less atmosphere to be crossed, leading to lower values of attenuation. A simple two columns table is then sufficient for the path loss caused by trophosperic scintillation, and provided in table 3.7.

| **Elevation angle [deg]** | **Tropospheric attenuation** |
|---|---|
| 10 | 1.08 dB |
| 20 | 0.48 dB |
| 30 | 0.30 dB |
| 40 | 0.22 dB |
| 50 | 0.17 dB |
| 60 | 0.13 dB |
| 70 | 0.12 dB |
| 80 | 0.12 dB |
| 90 | 0.12 dB |

Table 3.7: Attenuation values for tropospheri attenuation

### 3.2.7 Fast Fading

The 3GPP document on NTN offers a flat fading model for the channel, called the ITU two-state model. This model is tested (and works) for a bandwidth of 5MHz or less, together with LOS conditions and S-band frequencies, making it unusable for the purpose of simulating a variety of scenarios in the NTN environment. The description of the flat fading model is then omitted from this thesis, which implements the frequency selective model.
In the fast fading model for NTN, the process is the same as the one used in TR 38.901 [25] and described in chapter 2. The main difference is in the parameters of the fading model, which depend on the scenario, the propagation condition (LOS or NLOS), the frequency, as well as the elevation angle. The table of parameters for the fading is reported in [28], with numbers from 6.7.2-1a to 6.7.2-8b

### 3.2.8 Additional losses

The attenuation factors presented so far can be treated as main factors in the channel estimation process, and are almost always present. There are two types of additional signal degradation factors which, however, are not considered for system level simulations. The first one is the outside

to inside (O2I) penetration loss, which greatly varies with the location and construction characteristics of the building. A statistical evaluation method, based on thermal-efficency factors, is provided by 3GPPs and needs to be used if considering UEs placed inside of buildings. However, in this implementation of the channel model, only outdoor conditions are being considered.
The second attenuation factor (here neglected) is the one given by rain and clouds, and this choice comes from the recommendation by 3GPP to consider only clear-sky condition when performing system-level simulations.

### 3.2.9 Antenna models

Multiple antenna options are offered, depending on which type of device and conditions are being considered.
Regarding satellites options, 3GPP suggests a single model, the one of a circular aperture antenna. Circular aperture antennas are a type of reflector antennas that offer circular polarization, and which normalized antenna gain pattern is given by:

$$4\left|\frac{J_1\left(k \cdot a \cdot sin\theta\right)}{k \cdot a \cdot sin\theta}\right|^2 \qquad for\ 0 < |\theta| \leq 90^\circ \tag{3.5}$$

$$1 \qquad for\ \theta = 0 \tag{3.6}$$

Where $J_1()$ is the Bessel function of the first kind and first order, $a$ is the radius of the antenna's circular aperture, and given a frequency of operation $f$ the value $k$ is equal to $k = \frac{2\pi f}{x}$, with $c$ the speed of light in vacuum. This type of antennas feature a *symmetric* radiation patter, meaning that only one angle is enough to calculate the radiation strength in a certain direction, since only the angle $\theta$ from the bore sight is needed. Figure 3.8 depicts the radiation pattern of this antenna.

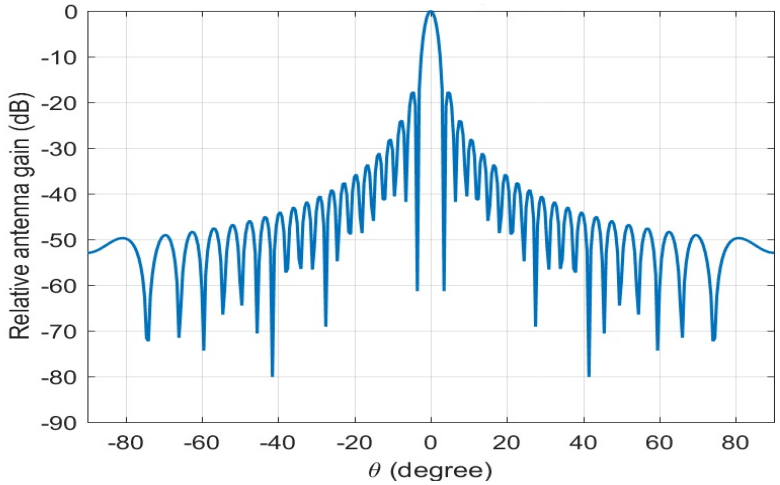


Figure 3.8: Circular aperture antenna relative gain pattern, for $a = 10c/f$. Image from [28]

When considering flying vehicles that are not satellites, such as HAPs and UAVs, the lower distance opens up for the possibility of an additional antenna choice. This corresponds to the UPA antenna model, already presented in chapter 2 and currently used as the standard antenna type for UE and e/gNB in the 3GPP 38.901 [25] document for terrestrial terminals.
Terminals on the ground instead, are left with two choices. The first one being the already seen UPA antenna model, and the second one being a very small aperture terminal (VSAT) antenna model. VSAT have been vastly used in satellite telecommunications, and are circular reflector antennas of small sizes (less than 1m of diameter), to be typically placed on roofs pointing at the sky. Their radiation pattern is the same as the one presented for circular aperture antennas in figure 3.8, and described by equation 3.5 and 3.6.

| | **Circular Aperture** | **UPA** | **VSAT** |
|---|---|---|---|
| **Satellite** | X | | |
| **HAPS/UAV** | X | X | |
| **UE** | | X | X |

Table 3.8: Possible antenna choices for every type of node

# Chapter 4

# NTN Implementation on NS-3

The implementation in NS-3 of the NTN channel model is built upon the existing 3GPP spacial channel model presented in [24]. The additional methods and classes have been created with the intention of extending NS-3 without compromising any of its functionalities, thus minimal change to existing classes is preferred. Nevertheless, some unavoidable modifications to the existing code structure are needed. Figure 4.2 contains a conceptual representation of the modifications and additions performed to the codebase.
The creation of the NTN channel model has followed the 3GPP [28] recommendations presented in chapter 3, which are considered a standard in the telecommunication landscape. Figure 4.1 summarizes the main steps in the channel creation as described by 3GPP which holds true for both terrestrial and NTN channel models.
In the first part of this chapter, an overview on NS-3 is given, highlighting its main characteristics. Subsequently, alterations of the existing code structure and additions of new components specifically tailored to NTNs are described.
The ns-3 source code, including the new NTN modifications introduced in this thesis, can be found at [36].

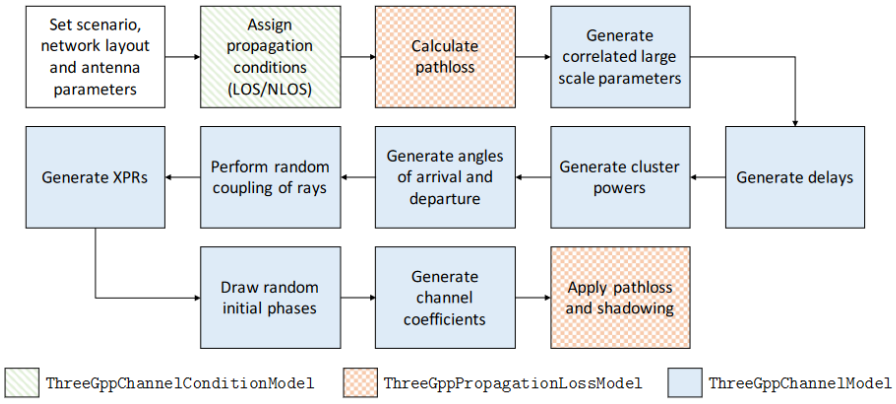


Figure 4.1: Channel Generation Procedure, from [24]

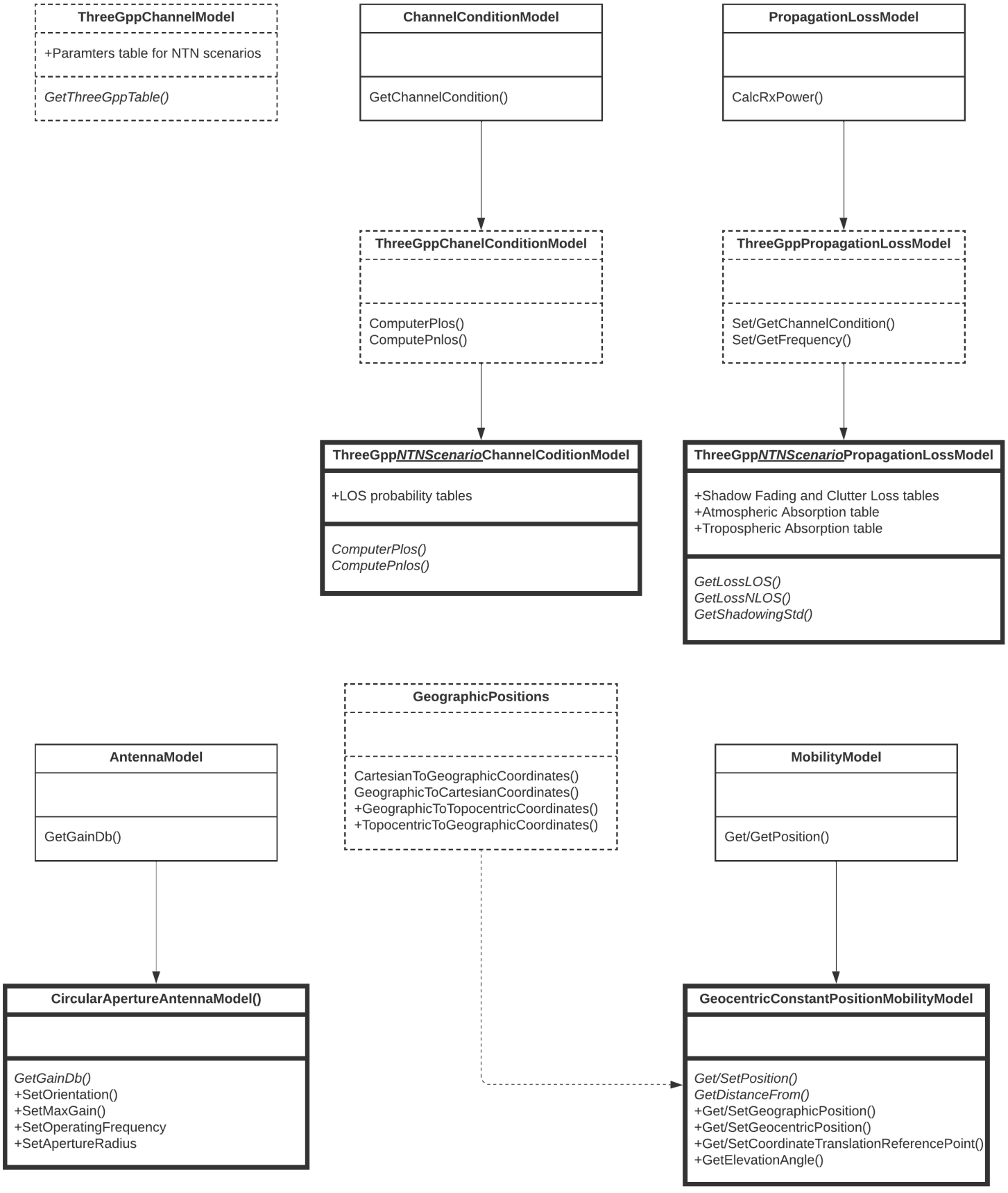


Figure 4.2: Class diagram of the NTN channel model implementation, with only significant methods displayed. Bold classes are newly implemented classes. Dotted classes are existing classes that have been modified

## 4.1 NS-3

NS-3 is a free and open-source network simulator, using a GNU GPL licensing [37], whose development started in 2006. It features discrete event scheduling, and it provides simulation support for full-stack simulations. While providing Python bindings, it's written in the C++ programming language, making it a fast and efficient software. NS-3 is currently supported, and a vast community contributes at keeping it up-to-date with the latest protocols, communication standards and network types. The main purpose for which NS-3 is being created is research and educational. NS-3 is extensible and upgradable by nature, with *modules* that extend support and functionalities.
Furthermore, notable efforts have been made to create modules able to effectively simulate NR technologies, including the one brought with 5G, such as mmWaves [24]. This makes NS-3 the obvious choice for the work of this thesis, since the implementation process can relay on existing classes and methods that are already built with the 3GPP channel model as reference.

### 4.1.1 Coordinate System

3GPP uses a Cartesian coordinate system comparable to the one adopted by 3GPP for terrestrial networks (presented in section 2.2.5) where the position of each node is uniquely described by three values $(x, y, z)$, with $x$ and $y$ spanning the ground plane, and $z$ indicating the height of a certain node. NS-3 uses a comparable coordinate system for the position of each UE and NB, but when considering arrival and departure angles at a specific antenna a different set of coordinates is implemented, which is composed of spherical coordinates. A generic point in spherical coordinates is described as $(r, \phi, \theta)$, but since the operations performed with these sets of coordinates concerns antenna field patterns, the radial component $r$ is dropped, leaving the *inclination* $\theta$ and *azimut* $\phi$.

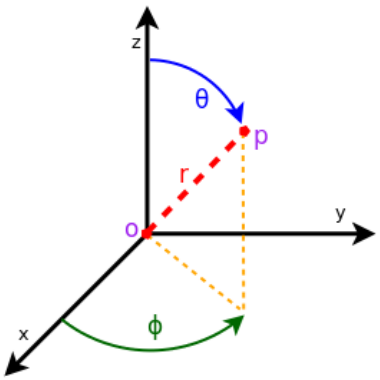


Figure 4.3: Polar coordinate or (LCS)

In the 3GPP TR [25] the Cartesian coordinates takes the name of global coordinate system (GCS), while the polar coordinates are named local coordinate system (LCS). A proper method of translation between the two system is required when using antenna's field patterns, and [25] describes the translation process currently implemented into the mmWave module of NS-3.

## 4.2 The ns-3 NTN channel

This section describes the NS-3classes that required some level of intervention to implement the newNTN channel model.

### `ThreeGppChannelModel`

This class is responsible for the calculation procedure that includes small scale parameters, described in section 7.5 of [25] and discussed in chapter 2. The procedure is the same as in the case of terrestrial networks, and corresponds to the one presented in section 2.2.7, but requires different parameters as discussed in section 3.2.7. A single parameter in the satellite channel model, has multiple factors that determine his value, namely: scenario, LOS conditions, frequency bands and elevation angles. Taking into consideration four scenarios, two LOS condition, two frequency band and nine elevation angle the final possible choices for a single parameters are 144. Given that the small scale parameters are more than 30 total values, a proper holding structure is needed to guarantee code efficiency and readability, bringing the choice to *nested maps*. To give an example, the map `NTNUrbanLOS` uses as key the frequency band (S or Ka), which is used to return another map that given the elevation angle contains the vector of the small scale parameters. This implicate the creation two maps for each scenario: one for the LOS case and one for the NLOS case, for a total of eight maps.
The signature of the `GetThreeGppTable()` method was changed to include the `MobilityModels` of transmitter and receiver nodes, due to the necessity of being aware of the elevation angle in order to get the correct small scale paramters. Further intervention to this class is the inclusion of additional angular scaling factors for scenarios that have lower number of clusters than the scenarios described in TR 38.901.

### `GeographicPositions`

Geographic coordinates are a common reference system to indicate a point on the surface of the Earth, with it's relative altitude from the ground. Any location on Earth can be referenced by a longitude, a latitude and an altitude, creating the triplet $(\phi, \lambda, h)$. This coordinate

system is the most commonly used by maps and navigation software. As discussed in section 4.1.1, 3GPP recommends the *Geocentric Cartesian* (or ECEF) coordinate system, of which this class offers conversion to and from.
Besides this conversion between these two spherical systems, another positioning standard must be supported: the one used by NS-3 and already presented in section 4.1.1. The conversion between a coordinate system that places a terminal on a location of the Earth to one in which the node position lays in a imaginary plane, raises the need for a *reference point* of translation. Coordinates that uses a reference point of origin are called *topocentric coordinates*, or east north up (ENU) coordinates. This conversion is implemented in the methods
`GeographicToTopocentricCoordinates` and
`TopocentricToGeographicCoordinates` of this class, and the procedure used is the one described in chapter 4 of [38].

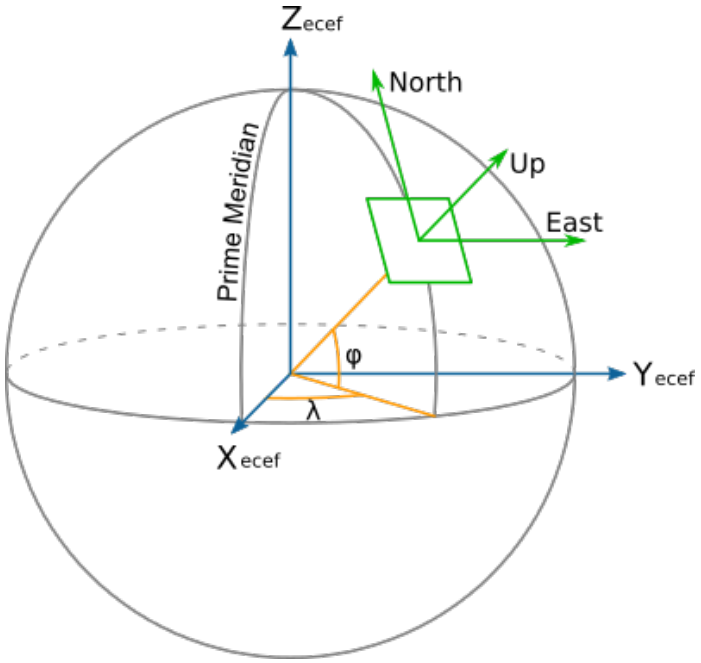


Figure 4.4: Geocentric Cartesian coordinates (or ECEF) compared to topocentric coordinates

## 4.3 Creation of new classes

This section presents the classes that have been introduced for the implementation of the NTN channel model.

### ThreeGppNTNScenarioChannelConditionModel

The `ChannelCondition` class was developed to store the channel state during the implementation performed by [24], together with the interface `ChannelConditionModel` that can be extended to implement any specific channel condition. The main method is `GetChannelCondition`, which given two mobility models returns a pointer to the corresponding `ChannelCondition`. To include the channel condition models for NTN scenarios, four different classes have been created, i.e.,

- `ThreeGppNTNDenseUrbanChannelConditionMode`
- `ThreeGppNTNUrbanChannelConditionMode`
- `ThreeGppNTNSuburbanChannelConditionMode`
- `ThreeGppNTNRuralChannelConditionMode`

each one derived from the same base class `ThreeGppChannelConditionModel` that extends itself `ChannelConditionModel`.
When the `GetChannelCondition` method is called the newly implemented classes calculate the channel state, with the procedure described in section 3.2.3, and the latter is stored together with the generation time, to be reused. When future channel state calculation requests are performed, the method check if the stored value is still valid based on the attribute `UpdatePeriod`, and if not the channel state is recalculated.

### ThreeGppNTNScenarioPropagationLossModel

Four different classes have been created, one for each possible scenario, all extending the `ThreeGppPropagationLossModel` class which itself extend the `PropagationLossModel` interface. These classes implements the process for the computation of the total pathloss. The main method of `PropagationLossModel` is `DoCalcRxPower`, that returns the received power based on the positions of the communicating nodes. The latter perform the power calculation using `GetLossLos`, `GetLossNlos` and `GetShadowing` to get the mean total pathloss. Since the shadowing loss is modeled as a log-normal random variable, it's calculation require the `GetShadowingStd` method, that returns the standard deviation value for a specific scenario.
The pathloss of an NTN scenario is composed of the basic free space

path loss, tropospheric and ionospheric scintillation, shadow fading, clutter loss and atmospheric absorption. The calculation methods of these effects has been discussed in chapter 3, but the implementation of the atmospheric absorption loss is not straightforward as taking values from a table. This is because the recommended method by 3GPP refers to values that are plotted into a scheme, and not available as raw data. Hence, the procedure used to implement atmospheric absorption loss is the following: (i) samples points are being manually extracted from figure 6 of [27], (ii) the extracted data is interpolated to increase the sampling rate, (iii) values of atmospheric absorption are extracted with 1GHz of step size, from 1 to 100GHz, and implemented as an array called `atmosphericAbsorption`.
The interpolation is performed using the *Piecewise Cubic Hermite Interpolating Polynomial (PCHIP)* algorithm [39]. Figure 4.5 shows the extracted and interpolated data.

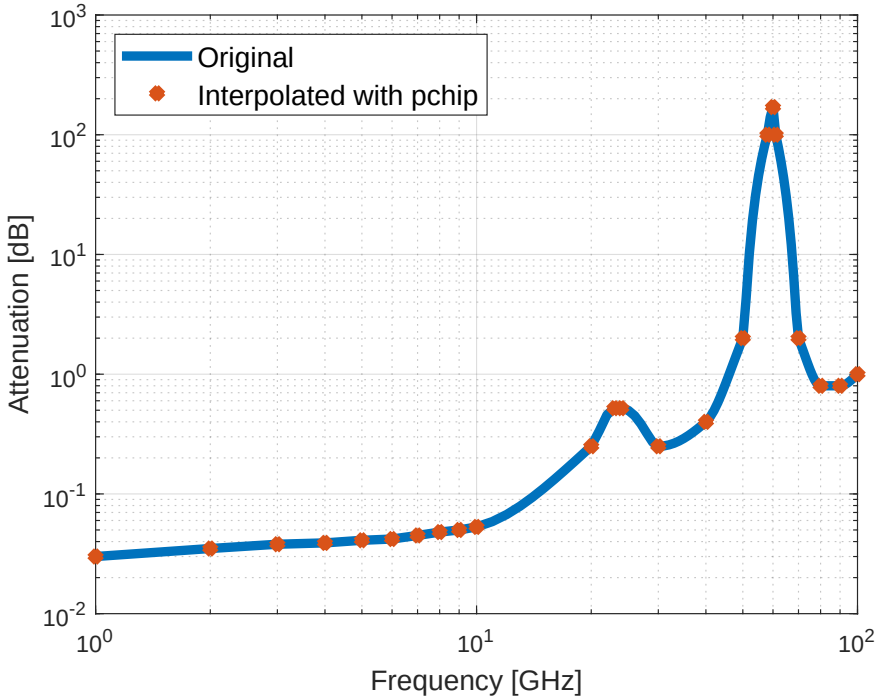


Figure 4.5: Interpolation of the atmospheric absorption values given by [27]

### `GeocentricConstantPositionMobilityModel`

The creation of a new mobility model, comes primarily from the need of calculating the elevation angle, which is essential in the estimate of many channel parameters as described in section 3.2. Additionally, having a mobility model that uses a coordinate system comparable to the ones

used in the real world brings many advantages, first of which, making the positioning of real world objects a more direct process. This class stores the position in the form of a variable containing geographic coordinates, named `m_position`, and can be obtained and set using the methods
`Set/GetGeographicPostion` and `Set/GetGeocentricPosition`. The latest use the methods offered and implemented in the class
`GeographicPosition` to perform translations between different coordinate systems.
The `GeocentricConstantPositionMobilityModel` class is derived from the base class `MobilityModel`, which imposes the presence of the
`Get/SetPosition()` methods, that are used to set and get the position of the object using Cartesian coordinates. Hence, conversion to and from this coordinates is crucial to maintain compatibility with the NS-3 code, as suggested directly by the developers in [40]. The conversion from geocentric Cartesian or geographic coordinates to the planar Cartesian coordinates largely used into NS-3 is performed relying again on the `GeograohicPosition` class, using as reference point for conversion $(0, 0, 0)$ (the *Null Island* [41]).
Additionally, the reference point for coordinates conversion can be set using `SetCoordinateTranslationReferencePoint`, making the values obtained when using `GetPosition()` more human readable.

### `CircularApertureAntennaModel`

NS-3 already contains an antenna model for circular aperture reflector antennas, called `ParabolicAntennaModel`, which however is based on a parabolic approximation of the main lobe radiation pattern, as presented in [42] and [43]. The latter is used mainly for the reduced computational complexity in the field pattern calculation, avoiding the use of the Bessel function that a circular aperture antenna requires, taking advantage of trigonometric functions. Since the introduction of C++17 however, an efficient implementation of the Bessel functions are provided directly into the `std` library, making the creation of an antenna model free of approximations more straight forward. Figure 4.6 is a comparison between the simplified field pattern and the complete one that is implemented.
`SetOperatingFrequency` and `SetApertureRadius` are used to input these values.

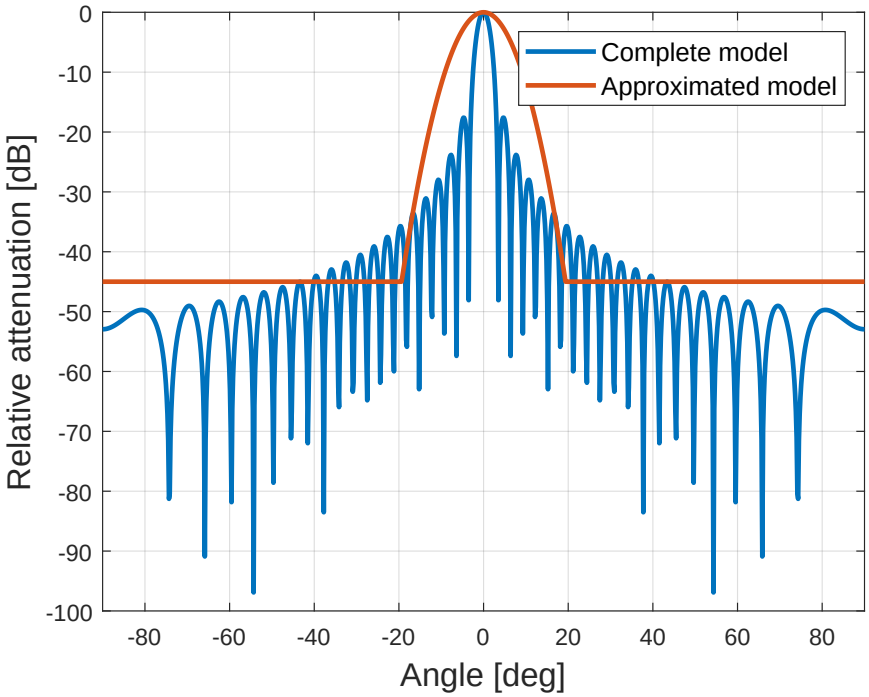


Figure 4.6: Circular aperture antenna: approximated versus complete field pattern

Hence the complete model for circular aperture antennas presented in chapter 3 is implemented as the `CircularApertureAntennaModel` class, inherited from the `AntennaModel` base class. This model offers antenna orientations options through the `SetOrientation` and `SetInclination` methods, and overrides the `GetGainDb` method of the base class using the proper field pattern calculation. Operating frequency and aperture radius are essential parameters to correctly estimate the radiation pattern of a circular aperture antenna, thus the methods `Get/SetOperatingFrequency` and `Set/GetApertureRadius` are created to allow for the input of these values.

# Chapter 5

# Simulation and Performance Evaluation

In this chapter, the implemented model is used to conduct a series of simulations and reporting the results obtained. Each simulation scenario is complemented by the parameters adopted. First, the set of parameters and possible scenarios are presented. Then, a discussion is performed regarding the outcomes of the experiments, which aims at identifying the possible causes that lead to those specific results. At the end, a consideration on what type of network configuration might be feasible or not is given.

## 5.1 Simulation Parameters

### 5.1.1 Scenarios

An assortment of thirty *scenarios* are proposed by 3GPP in [30], combining a multitude of possible variables. The carrier frequencies are fixed in the two bands of interest, the S-band at 2GHz and the Ka-band, which sets the Uplink frequency at 30GHz and the Downlink one at 20GHz. Orbit types are the one discussed in chapter 2, and the terminal refers to the antenna used by the ground device, choosing from the two options presented in chapter 3. Here the term *handheld* refers to a two-by-two UPA with linear polarization.
3GPP classifies the scenarios in three levels of descending priority, form the $1^{th}$ priority scenarios being the most possible real world use cases of an NTN network to the $3^{rd}$ being the least feasible. In this thesis only the first two level of priority are considered, reducing the overall number of configuration to fifteen. Table 5.2 lists the main characteristics for every scenarios.
Circular aperture are circularly polarized antennas, while handheld devices implementing UPA antennas use linear polarization, creating a *polarization mismatch* that causes the halving of the radio link budget (-3dB). Following this reasoning, one might think that this loss of power

due to polarization mismatch is not present if using two circularly polarized antennas, however this is not certain. Signal reflection and other phenomena can cause a right-handed circular polarization to become a left-handed one, and vice versa. In this regard 3GPP introduces a *polarization reuse* option, that mitigate this effect by combining the power received by two polarizations at the same terminal, suppressing the -3dB loss. The polarization reuse is indicated as "Option 2" when enabled and "Option 1" otherwise.

| **Terminal:** | **Handheld** | | **VSAT** | |
|---|---|---|---|---|
| **Polarization reuse:** | 1 | 2 | 1 | 2 |
| **S-band** | -3dB | 0 | X | X |
| **Ka-band** | X | X | -3dB | 0 |

Table 5.1: Radio link loss due to polarization mismatch for every combination of frequency, user's antenna and polarization reuse option

| **Case** | **Orbit** | **Terminal** | **Frequency Band** | **Polarization Reuse** |
|---|---|---|---|---|
| **1** | GEO | VSAT | Ka-band | Option 1 |
| **2** | GEO | VSAT | Ka-band | Option 2 |
| **3*** | GEO | VSAT | Ka-band | Option 2 |
| **4*** | GEO | Handheld | S-band | Option 1 |
| **5*** | GEO | Handheld | S-band | Option 2 |
| **6** | LEO-600 | VSAT | Ka-band | Option 1 |
| **7** | LEO-600 | VSAT | Ka-band | Option 2 |
| **8*** | LEO-600 | VSAT | Ka-band | Option 2 |
| **9** | LEO-600 | Handheld | S-band | Option 1 |
| **10** | LEO-600 | Handheld | S-band | Option 2 |
| **11*** | LEO-1200 | VSAT | Ka-band | Option 1 |
| **12*** | LEO-1200 | VSAT | Ka-band | Option 2 |
| **13*** | LEO-1200 | VSAT | Ka-band | Option 2 |
| **14** | LEO-1200 | Handheld | S-band | Option 1 |
| **15** | LEO-1200 | Handheld | S-band | Option 2 |

Table 5.2: Main parameters for each scenario. First priority scenarios have no *, while second priority ones have one *.

The channel bandwidth and resource block (RB) size for each frequency band is set according to table 5.3

| Frequency band | **Bandwidth** | **RB size** |
|---|---|---|
| **S band** | 30MHz | 60 kHz |
| **Ka band** | 400MHz | 240 kHz |

Table 5.3: Bandwidth and RB size for each frequency band

### 5.1.2 Satellite Parameters

Depending on orbit and altitude, 3GPP recommends different parameter sets, that regards the satellite antenna and are considered a baseline for simulations. The max gain is the gain that the circular aperture antenna of the satellite's payload achieves on the bore sight direction, while the equivalent antenna aperture is needed in order to get a correct estimate of the field pattern. Effective Isotropic Radiated Power (EIRP) density is the maximum power spectral density that the antenna can radiate, making the transmitted power value related to the bandwidth of the transmission. The value for the transmitted power, before antenna's amplification, can be obtained as:

$$\begin{aligned} TxPower\,[dBm] = EIRP_{density}\left[\frac{dBW}{MHz}\right] + \\ 10log_{10}\left(Bandwidth\,[MHz]\right) - \\ AntennaGain_{max}\,[dB] - 30 \end{aligned} \tag{5.1}$$

Tables from 5.4 to 5.7 gives the parameters for satellite antennas configuration.

| **Satellite orbit** | **GEO** | **LEO-1200** | **LEO-600** |
|---|---|---|---|
| **Satellite altitude** | 35786 km | 1200 km | 600 km |
| **Equivalent antenna aperture** | 22 m | 2 m | 2 m |
| **EIRP density** | 59 dBW/MHz | 40 dBW/MHz | 34 dBW/MHz |
| **Satellite max Gain** | 51 dBi | 30 dBi | 30 dBi |

Table 5.4: Satellite antenna parameters for Downlink simulations on the S-band 2GHz

| **Satellite orbit** | **GEO** | **LEO-1200** | **LEO-600** |
|---|---|---|---|
| **Satellite altitude** | 35786 km | 1200 km | 600 km |
| **Equivalent antenna aperture** | 5 m | 0.5 m | 0.5 m |
| **EIRP density** | 40 dBW/MHz | 10 dBW/MHz | 4 dBW/MHz |
| **Satellite max Gain** | 58.5 dBi | 38.5 dBi | 38.5 dBi |

Table 5.5: Satellite antenna parameters for Downlink simulations on the Ka-band 20GHz

| **Satellite orbit** | **GEO** | **LEO-1200** | **LEO-600** |
|---|---|---|---|
| **Satellite altitude** | 35786 km | 1200 km | 600 km |
| **Equivalent antenna aperture** | 22 m | 2 m | 2 m |
| **Satellite max Gain** | 51 dBi | 30 dBi | 30 dBi |

Table 5.6: Satellite antenna parameters for Uplink simulations on the S-band 2GHz

| Satellite orbit | GEO | LEO-1200 | LEO-600 |
|---|---|---|---|
| **Satellite altitude** | 35786 km | 1200 km | 600 km |
| **Equivalent antenna aperture** | 3.33 m | 0.33 m | 0.33 m |
| **Satellite max Gain** | 58.5 dBi | 38.5 dBi | 38.5 dBi |

Table 5.7: Satellite antenna parameters for Uplink simulations on the Ka-band 30GHz

### 5.1.3 UE Parameters

The antenna selection for the UE is dictated by the frequency band in use, with higher frequencies (Ka band) requiring a VSAT antennas to make communication possible. Table 5.8 collects the parameters to be used, recommended by 3GPP [30], for the UE equipment.

| - | VSAT | Handheld |
|---|---|---|
| Frequency band | Ka band | S band (i.e. 2 GHz) |
| Antenna configuration | Directional with 60cm aperture | omni-directional elements |
| Rx Antenna gain | 39.7 dBi | 0 dBi per element |
| Noise figure | 1.2 dB | 7 dB |
| Tx transmit power | 2 W (33 dBm) | 200 mW (23 dBm) |
| Tx antenna gain | 43.2 dBi | 0 dBi per element |

Table 5.8: UE antenna parameters

### 5.1.4 Assumptions

This section contains the assumption made during the test and perfomance evaluation of the implemented channel model.
A common metric used by 3GPP is the *Signal to Interference Noise Ration* SINR, calculated as such:

$$SINR_{dB} = 10 * log10\left(\frac{S}{N+I}\right) \tag{5.2}$$

Where $S$ is the received signal power, $N$ is the noise power and $I$ is the power coming from interference. However, in this thesis only one receiving and one transmitting terminals are considered at all time, bringing the interference power to always be zero. Hence, only signal to noise ratio (SNR) is used.
Another assumptions is that transmitting and receiving terminals are stationary at all time, thus Doppler effect due to moving nodes is considered not present.
When using UPAs, beamforming is required: in this thesis the DFT beamforming algorithm is used, which produces results similar to an ideal beamforming algorithm [44].

## 5.2 Simulation Campaign

In this section, simulations results are presented and discussed, using as main metrics the SNR and the total pathloss.

### 5.2.1 Calibration

Before moving to experimental simulations, a validation of the implemented model is required. 3GPP 38.821 [30] provides tables containing parameters to facilitate this process, together with simulation results to compare to. Table 5.9 show the obtained results.

| Case | mode | Frequency [GHz] | SNR [dB] | Obtained SNR [dB] |
|---|---|---|---|---|
| **SC1** | DL | 20.0 | 11.6 | 10.53 |
| | UL | 30.0 | 5.0 | 5.51 |
| **SC6** | DL | 20.0 | 8.5 | 9.52 |
| | UL | 30.0 | 18.4 | 21.17 |
| **SC9** | DL | 2.0 | 6.6 | 7.81 |
| | UL | 2.0 | 2.8 | 3.87 |
| **SC11** | DL | 2.0 | 6.6 | 6.54 |
| | UL | 2.0 | 2.8 | 3.89 |
| **SC14** | DL | 2.0 | 7.2 | 6.70 |
| | UL | 2.0 | -2.6 | -1.33 |

Table 5.9: Calibration results

Results obtained are in-line to the reference from [30], and small variations can be mainly attributed to: (i) the missing interference power in the SNR calculation, as discussed in 5.1.4. (ii) Reference simulations parameters being based on different versions of [28], which might bring changes according to the latest measurement campaigns and studies.

### 5.2.2 Simulations

In this section different simulations are performed, and their results presented and discussed, in order to investigate and give an overview of the simulations made possible as outcome of the implementation.

#### Elevation angle comparison

In this experiment, a satellite at an altitude of 600km is deplyed to measure pathloss and SNR values for different elevation angles. Changing the satellite position, but keeping its altitude from ground fixed, aims at simulating how the signal might be effected as a LEO satellite moves along its orbit.
The test is performed in DL on the S band using $45.55dBm$ of power for the transmission. Other parameters are according to table 5.4 for the

satellite and table 5.8 for the UE. The simulations is performed for every scenario. Figure 5.1 depicts the results.
The results shows how dramatically the elevation angle affects the signal, with SNR values that experience a immediate degradation when going from communicating with a satellite that is perfectly positioned to one that is slightly shifted. Elevation angle however, is not the only factor that changes, since the altitude from ground of the satellite is kept the same throughout the test, the distance between the communicating nodes is increasing with the diminishing of the elevation angle, with values reporterd in table 5.10
The sudden drop of SNR when decreasing the elevation angle is also attributed to the small half power beam width (HPBW), denoted by $\theta_{3dB}$, of the satellite antenna. For the parameters used in this simulation, and using the HPBW formula (from [45]):

$$\theta_{3dB} = \frac{70\lambda}{d} \tag{5.3}$$

the HPBW is only 5.2 degrees. Hence, moving outsite of the main antenna beam greatly reduces the signal strength, degrading the SNR.

| **Elev. angle:** | **90** | **80** | **70** | **60** | **50** | **40** | **30** | **20** | **10** |
|---|---|---|---|---|---|---|---|---|---|
| **Distance[km]:** | 599986 | 606739 | 633905 | 679448 | 754542 | 874988 | 1,05E+06 | 1,33E+06 | 1,84E+06 |

Table 5.10: Node distance for every elevation angle

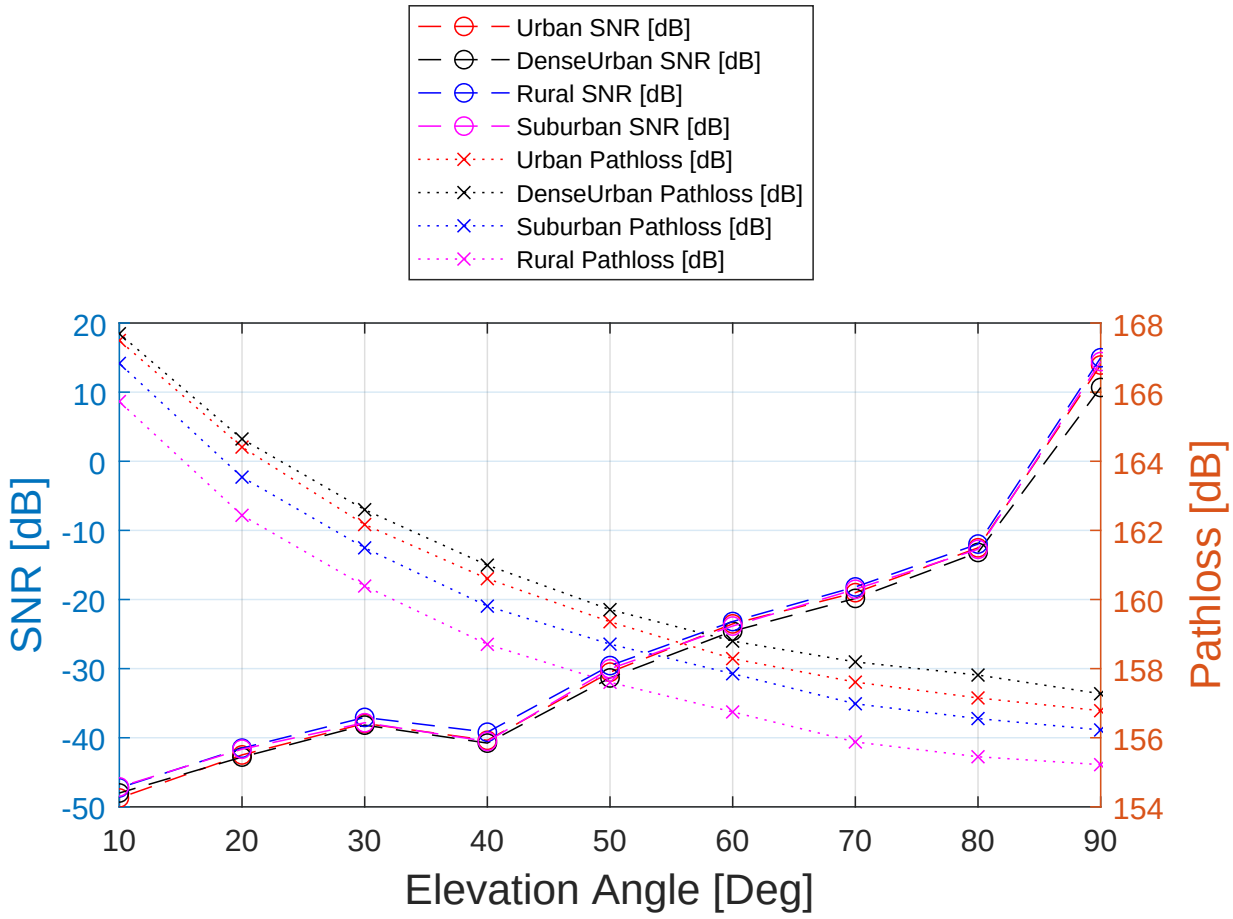


Figure 5.1: Pathloss and SNR as function of the elevation angle, for different scenarios

### LEO Altitude comparison

In this test, the effect of different altitude on the signal is studied for each frequency band. The scenario is set to rural. The experiment is performed for the two frequency bands of interest, and both in DL and UL. Parameters are set accordingly to 3GPP recommendations [28]. Table 5.11 contains the power figures used for each transmission. The altitude range spans from 300km to 2100km. Transmitting and receiving antenna powers and characteristics are the equal for each altitude.

| | S-band | | Ka-band | |
|---|---|---|---|---|
| Mode | **DL** | **UL** | **DL** | **UL** |
| Tx Power | **48.77dBm** | **29.0dBm** | **21.83dBm** | **33dBm** |

Table 5.11: Parameters used for the altitude comparison test

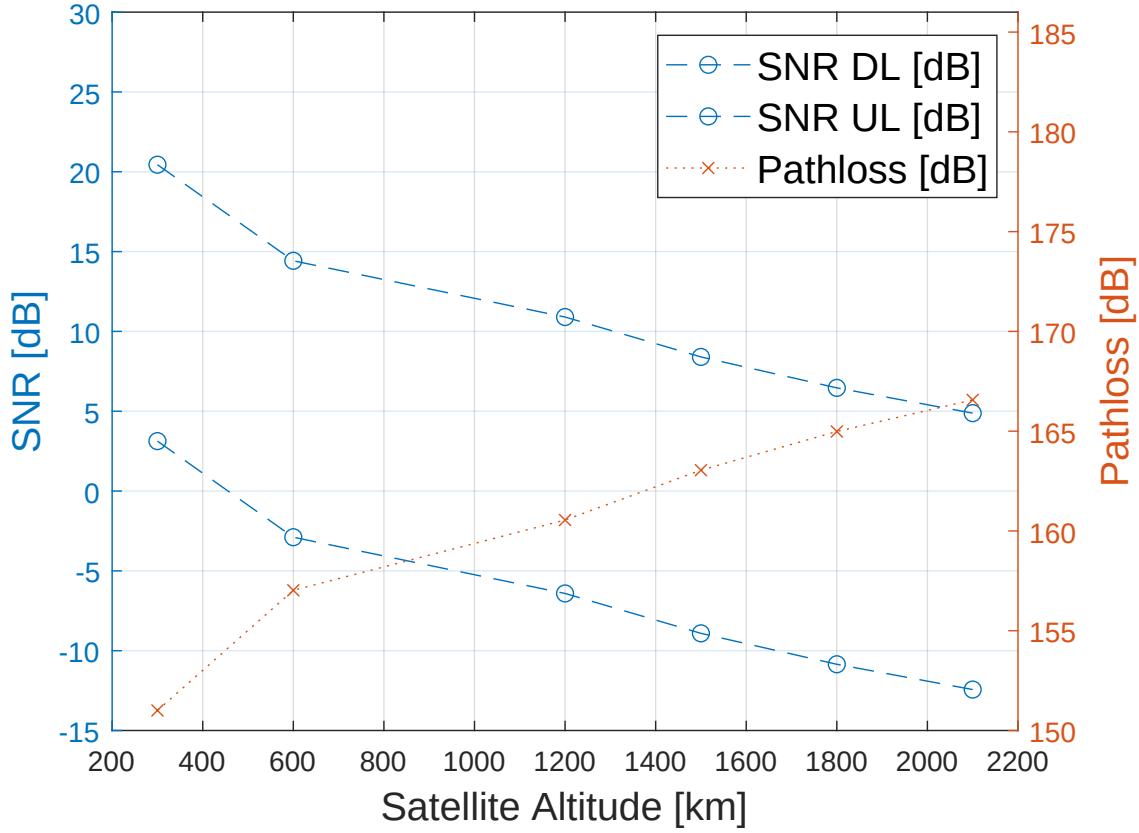


(a) Pathloss for different altitudes in the S band

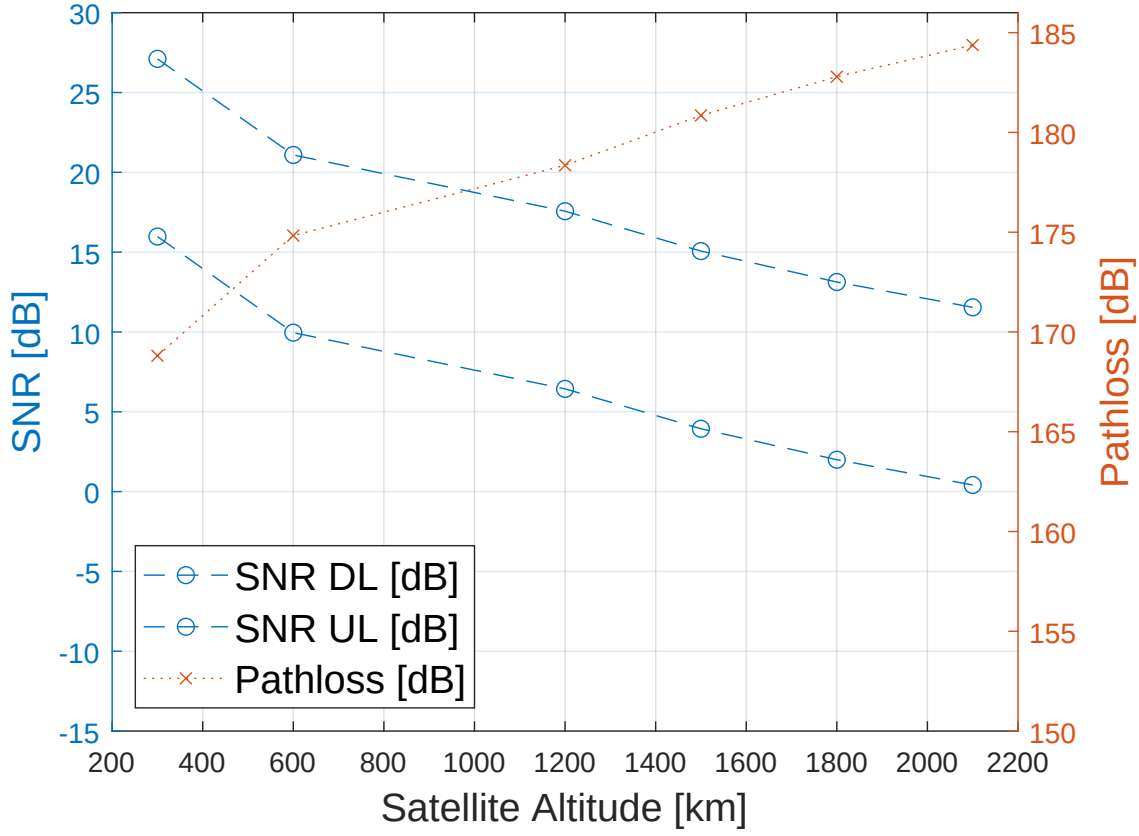


(b) Pathloss for different altitudes in the Ka band

Figure 5.2: Altitude versus pathloss compared between S band and Ka band.

Figure 5.2a and 5.2b contains the results obtained. The band using higher frequencies, i.e. the Ka band, is the one experiencing higher pathloss values, as expected. However, taking as example DL transmissions, SNR values are overall lower for the S band, despite the higher transmission power used. This is due to the VSAT antennas offering higher gain values with respect to handheld UPA antennas. Regarding UL transmission, the higher gain together with higher power usage of VSAT antennas help maintaining the SNR above the critical 0dB threshold for different values of the altitude, while UPA used in the S band manage to do so only at 300km from the ground. Having the SNR above the 0dB value is an indication that the received signal power is above the *noise floor*, under which communication is extremely limited.

**mmWaves for LEO satellites**

In this test, the feasibility of implement mmWaves for LEO satellite is tested. In the simulations performed so far, parameters have been configured according to the recommendations given by 3GPP in [28]. In this experiment however, case specific paramters are used, and summarized in table 5.12. This is because the use of an handheld device is supposed by the UE, reducing the gain available at the ground placed terminal with respect to the implementation of a VSAT antenna. This low level of received power can be partially or totally compensated by (i) deploying an antenna on the satellite side which offers higher gain or (ii) increasing the transmitted power.

| **Frequency:** | **Bandwidth:** | **RB size:** |
|---|---|---|
| 24GHz | 400MHz | 240kHz |

| **Orbit:** | **Altitude:** | **Polarization reuse:** |
|---|---|---|
| LEO | 600km | Option 1 (disabled) |

| **Satellite Antenna Gain:** | **Satellite Antenna Aperture:** | **Elevation angle:** |
|---|---|---|
| 49.65dBi | 1.5 m | 90 |

| **Satellite Antenna:** | **UE Antenna:** |
|---|---|
| Circular Aperture | Handheld (2x2 UPA) |

Table 5.12: Parameters used in the feasibility test of mmWaves

In regards to (i) we can suppose an high efficiency antenna on the satellite side that measures 1.5m of diameter, that at a frequency 24GHz and using the formula for the gain of a parabolic aperture antenna, given by:

$$G_{dB} = 10log_{10}\left(k\left(\frac{\pi D}{\lambda}\right)^2\right) \tag{5.4}$$

Leads to a maximum gain of $G_{dB} = 49.65dBi$. For what concerns (ii), multiple values of transmitted power are tested, spanning from 10W to 100W. Figure 5.3 depicts the results.

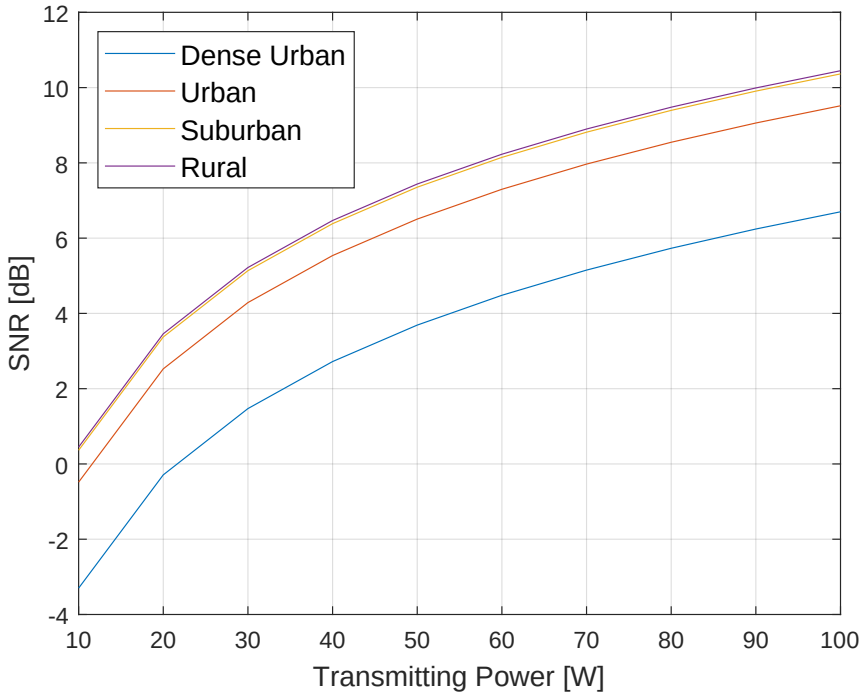


Figure 5.3: SNR as a function of the transmitted power for multiple scenarios

Transmission is always possible, even if close at the 0dB margin, for rural and suburban scenarios. Regarding the urban scenario, the received signal power is not sufficient to overcome the noise floor for low transmitting power, but the SNR value of 2dB is always surpassed for powers higher than 20W. The dense urban scenario represents the most challenging environment, where transmitted power needs to be brought over 30W to reach positive values of SNR.
The overall trend of the SNR curve is a logarithmic relation to the transmitted power.

### Full Stack Simulations

In this test, the complete 5G NR stack is simulated, to get an estimate of the possible capacity available at the application level provided by different configurations. The scenarios are chosen from the reference 3GPP simulation scenarios, described in [28] and reported section 5.1.1. The metrics considered are the application level throughput and the packet drop ratio, the latter defined as the ratio of packets that do not reach the destination to the total number of packets sent.
The application level at the transmitter side produces a constant bit rate

(CBR) data flow of 10Mbit/s, and packets are sent using the user datagram protocol (UDP). The environment's scenario is set to rural.
Results obtained are reported in table 5.13, together with some parameters that facilitate analysis.

| **Scenario:** | **1 GEO** | **6 LEO600** | **9 LEO600** | **14 LEO1200** |
|---|---|---|---|---|
| **Tx Power:** | 37.52 dBm | 21.52 dBm | 48.77 dBm | 54.77 dBm |
| **Tput:** | 3.811 Mbit/s | 3.286 Mbit/s | 4.101 Mbit/s | 5.161 Mbit/s |
| **Drop ratio** | 0.61 | 0.67 | 0.45 | 0.36 |
| **Frequency band:** | Ka-band | Ka-band | S-band | S-band |
| **UE terminal:** | VSAT | VSAT | Handheld | Handheld |

Table 5.13

All tested scenarios experience a high packet loss ratio(>0.3). Scenarios 1 and 9 are the most energy efficient, thanks to the high gain of the VSAT antennas implemented at the user's side. The results show that DL communication is possible from satellite to handheld devices, however, high transmission powers are required. For instance, satellites in scenario 6 and scenario 7 requires 75W and 300W of power, respectively, to achieve 4.1 and 5.1 Mbit/s throughput. This raises the issue of the power limit on satellites, imposed by on-board circuitry and batteries, which determines how frequent a spaceborne vehicle can provide this type of transmission before running out of energy.

### 5.2.3 Design Guidelines

This sections perform some considerations on the possible viable options offered by NTNs.
The preferable scenario for the establishment of a satellite internet communication, is a satellite in LEO orbits at 600km of altitude, together with a fixed VSAT antenna on the ground terminal. This is because the use of an high gain parabolic antenna on both sender and receiver nodes helps overcome the high pathloss introduced by the NTN environment.
A LEO satellite that orbits at 1200km brings the advantage of a greater coverage area on the ground and a higher service lifespan (as discussed in section 3.1.2), requiring however greater transmitting power and/or higher gain antennas.
The constant service availability offered by GEO satellites is available thanks to the use of big (>5m) diameter antennas on the spaceborne vehicles, which make communication at this distances from the ground (35786km) possible. Delay times, even if not treated in this thesis, are a physical barrier that poses limits on the use cases possible for LEO constellations.
Communication between satellite and handheld devices is feasible even for transmitting power of less than 40W using high gain antennas (>45dB),

and performance might be enhanced with polarization reuse implemented on portable devices.

# Chapter 6

# Conclusions

This thesis proposed an implementation of the 3GPP NTN channel model for NS-3.
After giving an overview of the novel concepts introduced by 5G, the main characteristics of its channel model are discussed.
NTNs are then introduced, highlighting possible use cases and improvements that might be brought by them to the present and future of 5G networks, together with the challenges they pose.
The possible deployment options that concern spaceborne and aerial vehicles have been introduced, discussing the pros and cons that each type of orbits or flying vessel offers, and how they have been typically adopted.
The NTN channel model provided by 3GPP is analyzed, including a comparison with the channel model for terrestrial networks, with a focus on the additional factors that concerns communication systems design outside the ground infrastructure.
Then, the contribution of this thesis is presented, describing the implementation process of the NTN channel model into NS-3, motivating the choices made during the development.
In the last chapter, a validation of the implemented model is done, comparing the obtained results with reference documents. Subsequently, the results from the simulation campaign performed are presented, showing that NTN might be a viable option for the extension of present and future network infrastructures. A discussion on the obtained results is then given.
At last, reference guidelines for possible implementation scenarios are proposed, highlighting the most promising use cases based on the simulation campaing results.
Nevertheless, additional research effort is required to gather additional information on the possibilities offered by NTN. In this regard, one of the possible improvements that could be brought in the future to this work is the consideration of the delays introduced by the long distances present in space scenarios, that can help identify criticalities that currently adopted protocols might encounter when dealing with NTN.

# Bibliography


[1] Telefonaktiebolaget LM Ericsson. "Mobile network traffic Q2 2022". In: (2022). DOI: https://www.ericsson.com/4a4be7/assets/local/reports-papers/mobility-report/documents/2022/ericsson-mobility-report-q2-2022.pdf.

[2] Telefonaktiebolaget LM Ericsson. *Mobile data traffic outlook*. URL: https://www.ericsson.com/en/reports-and-papers/mobility-report/dataforecasts/mobile-traffic-forecast.

[3] 3GPP. "Technical Release 21.917, Technical Specification Group Services and System Aspects, Release 17 Description, Summary of Rel-17 Work Items". In: (2022). DOI: https://portal.3gpp.org/desktopmodules/Specifications/SpecificationDetails.aspx?specificationId=3937.

[4] Marco Giordani and Michele Zorzi. "Non-Terrestrial Networks in the 6G Era: Challenges and Opportunities". In: *IEEE Networks* 35.2 (2021), pp. 244–251. DOI: https://arxiv.org/pdf/1912.10226.pdf.

[5] Wikipedia. *Satellite Internet Constellation*. URL: https://en.wikipedia.org/wiki/Satellite_internet_constellation.

[6] Thomas G. Roberts. "Space Launch to Low Earth Orbit: How Much Does It Cost?" In: (). DOI: https://aerospace.csis.org/data/space-launch-to-low-earth-orbit-how-much-does-it-cost/.

[7] Yunchou Xing et al. "High Altitude Platform Stations (HAPS): Architecture and System Performance". In: *2021 IEEE 93rd Vehicular Technology Conference (VTC2021-Spring)*. 2021, pp. 1–6. DOI: 10.1109/VTC2021-Spring51267.2021.9448899.

[8] Yongjae Kim et al. "5G K-Simulator: 5G System Simulator for Performance Evaluation". In: *2018 IEEE International Symposium on Dynamic Spectrum Access Networks (DySPAN)* (2018), pp. 1–2.

[9] Martin Müller et al. "Flexible multi-node simulation of cellular mobile communications: the Vienna 5G System Level Simulator". In: *EURASIP Journal on Wireless Communications and Networking* 2018 (Sept. 2018). DOI: 10.1186/s13638-018-1238-7.

[10] Giovanni Nardini et al. “Simu5G: A System-level Simulator for 5G Networks”. In: July 2020. DOI: 10.5220/0009826400680080.

[11] S. Martiradonna et al. “5G-air-simulator: an open-source tool modeling the 5G air interface”. In: (Apr. 2020). DOI: https://doi.org/10.1016/j.comnet.2020.107151.

[12] 3GPP. “5G NR Physical channels and modulation v16.10.0”. In: (2022). DOI: https://portal.3gpp.org/desktopmodules/Specifications/SpecificationDetails.aspx?specificationId=3213.

[13] Natale Patriciello et al. “5G New Radio Numerologies and their Impact on the End-To-End Latency”. In: (2018). DOI: https://ieeexplore.ieee.org/document/8514979.

[14] ETSI. *ETSI Standard for NFV*. URL: https://www.etsi.org/technologies/nfv.

[15] Sundeep Rangan, Theodore S. Rappaport, and Elza Erkip. “Millimeter-Wave Cellular Wireless Networks: Potentials and Challenges”. In: (2014). DOI: https://ieeexplore.ieee.org/abstract/document/6732923.

[16] Zhouyue Pi and Farooq Khan. “An Introduction to Millimeter-Wave Mobile Broadband Systems”. In: (2011). DOI: https://ieeexplore.ieee.org/document/5783993.

[17] Jonathan Lu et al. “Modeling Human Blockers in Millimeter Wave Radio Links”. In: (2012).

[18] M.A. Jensen and J.W. Wallace. “A review of antennas and propagation for MIMO wireless communications”. In: *IEEE Transactions on Antennas and Propagation* 52.11 (2004), pp. 2810–2824. DOI: 10.1109/TAP.2004.835272.

[19] Xiang Gao et al. “Massive MIMO Performance Evaluation Based on Measured Propagation Data”. In: *IEEE Transactions on Wireless Communications* 14.7 (2015), pp. 3899–3911. DOI: 10.1109/TWC.2015.2414413.

[20] Sooyoung Hur et al. “Proposal on Millimeter-Wave Channel Modeling for 5G Cellular System”. In: *IEEE Journal of Selected Topics in Signal Processing* 10.3 (2016), pp. 454–469. DOI: 10.1109/JSTSP.2016.2527364.

[21] Timothy A. Thomas et al. “3D mmWave Channel Model Proposal”. In: *2014 IEEE 80th Vehicular Technology Conference (VTC2014-Fall)*. 2014, pp. 1–6. DOI: 10.1109/VTCFall.2014.6965800.

[22] Ibrahim A. Hemadeh et al. “Millimeter-Wave Communications: Physical Channel Models, Design Considerations, Antenna Constructions, and Link-Budget”. In: *IEEE Communications Surveys & Tutorials* 20.2 (2018), pp. 870–913. DOI: 10.1109/COMST.2017.2783541.

[23] M. R. Akdenize et al. “Millimeter wave channel modeling and cellular capacity evaluation”. In: (2014). DOI: https://ieeexplore.ieee.org/document/6834753.

[24] Tommaso Zugno et al. “implementation of A Spatial Channel Model for ns-3”. In: (2020). DOI: https://arxiv.org/abs/2002.09341.

[25] 3GPP. “5G Study on channel model for frequencies from 0.5 to 100 GHz V16.1.0”. In: (2020). DOI: https://portal.3gpp.org/desktopmodules/Specifications/SpecificationDetails.aspx?specificationId=3173.

[26] Farooq Khan and Zhouyue Pi. “mmWave Mobile Broadband (MMB): Unleashing the 3-300GHz Spectrum”. In: (2011). DOI: https://ieeexplore.ieee.org/stamp/stamp.jsp?tp=&arnumber=5876482.

[27] International Telecommunication Union. “P.676 : Attenuation by atmospheric gases and related effects”. In: (2013). DOI: https://www.itu.int/rec/R-REC-P.676.

[28] 3GPP. “Technical Reprot 38.811, Release 15. Study on New Radio (NR) to support non-terrestrial networks”. In: (2020). DOI: https://portal.3gpp.org/desktopmodules/Specifications/SpecificationDetails.aspx?specificationId=3234.

[29] Xingqin Lin et al. “5G from Space: An Overview of 3GPP Non-Terrestrial Networks”. In: (2021). DOI: https://arxiv.org/ftp/arxiv/papers/2103/2103.09156.pdf.

[30] 3GPP. “Technical Specification Group Radio Access Network. Solutions for NR to support non-terrestrial networks (NTN)”. In: (2019). DOI: https://portal.3gpp.org/desktopmodules/Specifications/SpecificationDetails.aspx?specificationId=3525.

[31] Yannick Borthomieu. *Satellite Lithium-Ion Batteries*. URL: https://www.sciencedirect.com/science/article/pii/B9780444595133000145.

[32] Mohsen Hosseinian et al. “Review of 5G NTN Standards Development and Technical Challenges for Satellite Integration With the 5G Network”. In: *IEEE Aerospace and Electronic Systems Magazine* 36.8 (2021), pp. 22–31. DOI: 10.1109/MAES.2021.3072690.

[33] Marco Giordani and Michele Zorzi. “Non-Terrestrial Networks in the 6G Era: Challenges and Opportunities”. In: *IEEE Network* 35.2 (2021), pp. 244–251. DOI: 10.1109/MNET.011.2000493.

[34] Stephen Farrell et al. “When TCP Breaks: Delay- and Disruption-Tolerant Networking”. In: (2006). DOI: https://ieeexplore.ieee.org/stamp/stamp.jsp?tp=&arnumber=1704758.

[35] International Telecommunication Union. "P.531 : Ionospheric propagation data and prediction methods required for the design of satellite services and systems". In: (2012). DOI: https://www.itu.int/dms_pubrec/itu-r/rec/p/R-REC-P.531-11-201202-S!!PDF-E.pdf.

[36] Sandri Mattia. *3GPP NTN Channel Model Implementation into ns-3*. https://gitlab.com/mattiasandri/ns-3-ntn/-/tree/ntn-dev. 2022.

[37] Free Software Foundation. *General Public License*. URL: https://www.gnu.org/licenses/gpl-3.0.html.

[38] International Association of Oil and Gas Producers. "Geomatics Guidance Notes 7, part 2: Coordinate Conversions and Transformations including Formulas". In: (2021). DOI: https://www.iogp.org/bookstore/product/coordinate-conversions-and-transformation-including-formulas/.

[39] F. N. Fritsch and R. E. Carlson. "Monotone Piecewise Cubic Interpolation." In: 17.2 (1980), pp. 238–2461.

[40] NS-3. *Mobility Model on NS-3*. URL: https://www.nsnam.org/docs/models/html/mobility.html.

[41] Wikipedia. *Null Island*. URL: https://en.wikipedia.org/wiki/Null_Island.

[42] 3GPP. "Simulation assumptions and parameters for FDD HeNB RF requirements". In: (2009). DOI: https://www.3gpp.org/ftp/tsg_ran/WG4_Radio/TSGR4_51/Documents/.

[43] G. Calcev and M. Dillon. "Antenna tilt control in CDMA networks". In: (2006). DOI: https://dl.acm.org/doi/10.1145/1234161.1234186.

[44] D. Yang, L.-L. Yang, and L. Hanzo. "DFT-Based Beamforming Weight-Vector Codebook Design for Spatially Correlated Channels in the Unitary Precoding Aided Multiuser Downlink". In: *2010 IEEE International Conference on Communications*. 2010, pp. 1–5. DOI: 10.1109/ICC.2010.5502350.

[45] R. Straw and Ed Dean. *The ARRL Antenna Book, 19th Ed.* American Radio Relay League, 2000.